Heliyon 10 (2024) e35007

Contents lists available at ScienceDirect

Heliyon

journal homepage: www.cell.com/heliyon

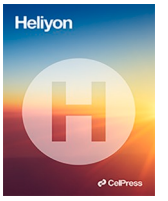

Review article

Musculoskeletal modeling and movement simulation for structural hip disorder research: A scoping review of methods, validation, and applications

Margaret S. Harrington [a], Stefania D.F. Di Leo [a], Courtney A. Hlady [a,b], Timothy A. Burkhart [a,*]

[a] Faculty of Kinesiology and Physical Education, University of Toronto, Toronto, ON, Canada
[b] Department of Physical Therapy, University of Toronto, Toronto, ON, Canada

ARTICLE INFO

Keywords:
Musculoskeletal modeling
Hip
Hip contact forces
Electromyography

ABSTRACT

Musculoskeletal modeling is a powerful tool to quantify biomechanical factors typically not feasible to measure *in vivo*, such as hip contact forces and deep muscle activations. While technological advancements in musculoskeletal modeling have increased accessibility, selecting the appropriate modeling approach for a specific research question, particularly when investigating pathological populations, has become more challenging. The purposes of this review were to summarize current modeling and simulation methods in structural hip disorder research, as well as evaluate model validation and study reproducibility. MEDLINE and Web of Science were searched to identify literature relating to the use of musculoskeletal models to investigate structural hip disorders (i.e., involving a bony abnormality of the pelvis, femur, or both). Forty-seven articles were included for analysis, which either compared multiple modeling methods or applied a single modeling workflow to answer a research question. Findings from studies comparing methods were summarized, such as the effect of generic versus patient-specific modeling techniques on model-estimated hip contact forces or muscle forces. The review also discussed limitations in validation practices, as only 11 of the included studies conducted a validation and used qualitative approaches only. Given the lack of information related to model validation, additional details regarding the development and validation of generic models were retrieved from references and modeling software documentation. To address the wide variability and under-reporting of data collection, data processing, and modeling methods highlighted in this review, we developed a template that researchers can complete and include as a table within the methodology section of their manuscripts. The use of this table will help increase transparency and reporting of essential details related to reproducibility and methods without being limited by word count restrictions. Overall, this review provides a comprehensive synthesis of modeling approaches that can help researchers make modeling decisions and evaluate existing literature.

1. Introduction

Musculoskeletal (MSK) modeling is a powerful tool that allows for the quantification of biomechanical factors that are generally not

* Corresponding author. Faculty of Kinesiology and Physical Education, University of Toronto, 55 Harbord Street, Toronto, ON M5S 2W6 Canada.
E-mail address: timothy.burkhart@utoronto.ca (T.A. Burkhart).

https://doi.org/10.1016/j.heliyon.2024.e35007
Received 11 July 2024; Accepted 22 July 2024
Available online 22 July 2024

feasible to measure *in vivo* [1,2]. Important insights into the potential causes and treatments of orthopaedic disorders have been generated from MSK modeling. For example, modeling studies have been performed to determine the effect of bone abnormalities on hip contact forces (HCFs) and how these may contribute to the progression and outcomes of femoroacetabular impingement syndrome (FAIS) [3], hip dysplasia [4], and hip osteoarthritis [5]. In addition, MSK modeling provides the ability to simulate treatments [6], potentially accelerating the translation of scientific findings into clinical practice and to facilitate more personalized treatment planning [7].

Technological advancements in MSK modeling have provided researchers with many choices for modeling and simulation [7]. While this has made MSK modeling more accessible, it has also increased the challenge for researchers to decide which assumptions, limitations, and uncertainties are acceptable to address their research questions [2,8]. Several recent reviews have synthesized the MSK modeling literature and have highlighted broad considerations for these modeling decisions [2,8–11] and emphasized a key challenge of MSK modeling; optimization of MSK modeling complexity (e.g., model personalization, muscle sets, approach for estimating muscle activations). In this case, optimizing complexity means the model needs to maximize anatomical accuracy while minimizing computational costs.

Different pathological populations may require unique model parameter selection and adjustments, which may further differ when modeling healthy controls. As well, when modeling structural hip disorders (i.e., bony deformities on the pelvis or femur), the bony geometry, hip joint centres, and muscle parameters can be represented by either generic models (derived from the geometry of healthy individuals [12]) or patient-specific models [13]. While general recommendations have been made for model validation, such as comparing model outputs against experimental data (e.g., instrumented prostheses, electromyography) [2,8], it remains unclear what the validation standards should be for specific populations and research questions. Furthermore, a recent review described studies that used MSK models to calculate hip joint loads in both healthy and pathological populations [14]; however, it did not include studies with other modeling outcomes such as muscle forces and moment arms, or that discussed model validation methods, or report details related to reproducibility.

Therefore, the purposes of this scoping review were to: i) summarize current modeling and simulation methods in structural hip disorder research; ii) describe model validation practices; and iii) highlight current issues related to study reproducibility. This review provides a comprehensive synthesis of evidence, which can assist researchers in evaluating modeling approaches used in existing or future studies. Key research priorities were also identified related to hip modeling to improve the results' reliability, reproducibility, and clinical relevance.

2. Methods

2.1. Search strategy

The search strategy was developed with the support of a professional librarian at the University of Toronto. The electronic databases MEDLINE and Web of Science were searched to identify relevant studies. The complete search strategies for each database are presented in Appendix A. In summary, the search strategies included keywords related to three search concepts: i) MSK modeling (e.g., models and simulations); ii) hip (e.g., pelvis and femur); and iii) structural disorder (e.g., disorder, pathology, and abnormality). This search strategy was developed based on a set of relevant studies that met the inclusion criteria. The retrieval of an additional set of pre-identified articles that met the inclusion criteria was used to validate the search strategy. Studies were retrieved up to July 3rd, 2023.

2.2. Inclusion and exclusion criteria

Studies were included if they developed or analyzed an MSK model to investigate a structural hip disorder. For this scoping review, a structural hip disorder was defined as any bony abnormality of the femoral neck, femoral head, or acetabulum [15]. MSK modeling was defined as a computational representation of the muscular system acting on a rigid, multibody skeletal structure [2]. Studies were excluded if: i) anatomical hip joint structures were not modeled or analyzed (e.g., they only investigated the effect of a prosthesis); ii) the experimental data collection included the use of walking aids (e.g., crutches, braces); iii) a non-human population was investigated; iv) it was written in a language other than English; and v) it was published as a conference proceeding only.

2.3. Study selection

Study duplicates from the search results were removed in EndNote before uploading the titles and abstracts to an online screening platform (Covidence 2023, Melbourne, Australia). Two of three independent reviewers screened all titles and abstracts of records for inclusion and exclusion. Then, two of three independent reviewers screened the full-text reports for studies included in the title and abstract screening step. Conflicts were resolved by a third reviewer (TB) at both stages of the screening process.

2.4. Quality assessment

A previously developed checklist for biomechanics research was used to assess the included studies' quality (Appendix B) [16]. The articles were scored for each question based on no (zero points), limited (one point), or satisfactory (two points) information, and the overall score was calculated as the sum of points divided by the maximum potential score for applicable questions [16]. A sub-sample of three studies was evaluated by two authors (MH, TB) and disagreements were discussed and resolved between the two assessors to

reach a consensus on the interpretation of the quality assessment. For this study, the checklist was modified to include the question: "Were relevant instrumentation specifications and signal processing techniques described?" In addition, the questions "Was the evaluation strategy appropriately justified?" and "Were the analytical methods clearly described?" were removed because the other questions and the analysis conducted for the scoping review expanded on these areas of the studies. The evaluation of each study was then conducted by one author (MH).

2.5. Data extraction

Based on established guidelines from Arksey and O'Malley [17], a data chart form in Microsoft Excel (Version 16.70, Microsoft Corporation, Redmond, USA) was developed to extract the required information for analysis, including the authors, publication date, sample demographics, primary study objective, main results, MSK model characteristics (and any alterations if a generic model was used), experimental inputs, simulation outputs, and validation procedures. Two of the three authors (MH, SD, CH) completed data extraction for each article, and disagreements were resolved in a discussion meeting. The data was then collated into the results tables and summarized [17]. Lastly, the authors analyzed the tables to identify key issues and themes related to the MSK modeling methods and applications [17]. If the models were incompletely described, details regarding MSK model characteristics or alterations to generic models were retrieved from references, the OpenSim modeling software (Stanford University, Stanford, USA) documentation [18], or the AnyBody Modeling System (AnyBody Technology, Aalborg, Denmark) [19].

3. Results

3.1. Search results

A total of 1525 articles were retrieved from the database searches and 47 were retained for analysis (Fig. 1). The results of the quality assessment are reported in Appendix B (Table B1). Summaries of the study characteristics and population demographics are provided in Tables 1 and 2, respectively. The hip disorders investigated in the included studies were osteoarthritis (n = 15), hip dysplasia (n = 11), cerebral palsy-associated femoral deformities (n = 8), FAIS (n = 9), and idiopathic femoral version deformities (n = 4) (Table 1). Gait (i.e., level walking) was the most common movement simulated (n = 36). Ten studies included simulations of more demanding and hip-provocative tasks, such as double and single leg squats (n = 5), stair climbing (n = 4), isolated hip range of motion (n = 3), and rehabilitation exercises (i.e., hip-focused with lower-extremity and trunk strengthening and stretching) (n = 1).

The included studies primarily implemented MSK modeling to quantify HCFs (n = 39) and muscle forces or activations (n = 22) (Table 1). The main outcomes of interest reported also included parameters related to muscle paths and capacities (e.g., moment arms, moment generating capacity), hip joint centre locations, joint angles and moments, and muscle co-contraction indices. Three studies

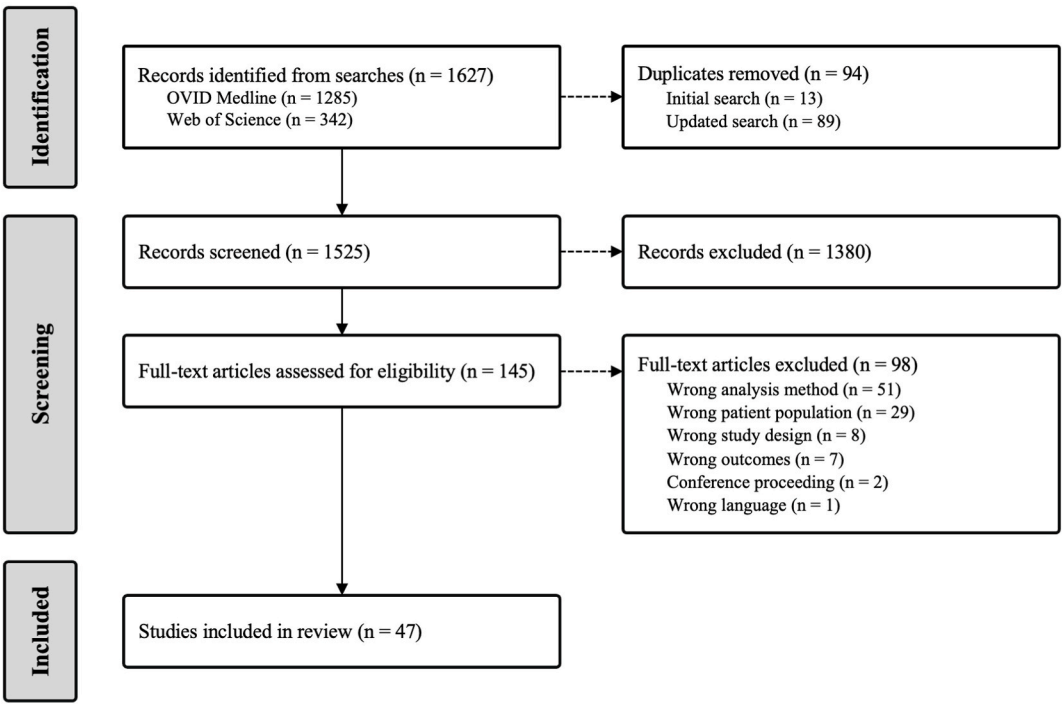

Fig. 1. PRISMA flow chart.

Table 1
Overview of included studies' independent variables, movement tasks simulated, and main model outputs of interest.

Focus	Reference	Independent Variable	Movement Task	Model Outputs
Osteoarthritis	Bahl et al. [20]	PS geometry	Simulated hip range of motion	HJC, MMA
	Bahl et al. [5]	THA	Gait	HCF
	Buehler et al. [21]	Exercise resistance, task	Rehabilitation exercises, gait	HCF, MF
	Diamond et al. [22]	Hip condition	Gait	HCF, MF, muscle co-contractions
	Foucher et al. [23]	Hip condition, THA	Stairs	HCF
	Fuller and Winters [24]	Arthritis Foundation's Exercise Program	Rehabilitation exercises	HCF
	Hoang et al. [25]	Control model	Gait	HCF, muscle co-contractions
	Lenaerts et al. [26]	PS geometry, simulated geometry & weakness	Gait	HCF, MF
	Lenaerts et al. [27]	PS geometry	Gait	HCF, muscle moments
	Lenaerts et al. [28]	THA	Gait	HCF
	Meyer et al. [29]	Hip condition	Gait	HCF, MF
	Wesseling et al. [30]	PS maximum isometric muscle forces, THA	Gait, stairs	HCF, hip moment generating capacities
	Wesseling et al. [31]	Hip condition, THA	Gait	HCF
	Wesseling et al. [32]	PS load inputs for finite element models	Gait	HCF
	Van Rossom et al. [33]	Hip condition	Gait, stairs	HCF
Hip dysplasia	Delp et al. [34]	Simulated osteotomy	Simulated hip range of motion	Muscle moments
	Gaffney et al. [35]	Simulated osteotomy	Gait	HCF, MF, MMA
	Gaffney et al. [6]	Simulated rehabilitation	Single leg squat	HCF, MF
	Harris et al. [36]	Hip condition	Gait	HCF, MF
	Song et al. [13]	PS geometry	Gait	HCF, MF, HJC, hip angles & moments
	Song et al. [37]	Hip condition	Gait	HCF, MF, MMA, muscle lines of action
	Song et al. [38]	Hip condition	Gait	HCF
	Song et al. [4]	Hip condition	Squat	HCF
	Shepherd et al. [39]	Simulated femoral version	Gait	HCF, MF, MMA, hip angles
	Shepherd et al. [40]	Simulated osteotomy	Gait	HCF, MF
	Wu et al. [41]	Hip condition	Gait	HCFs, HJC, MMA
Cerebral palsy	Bosmans et al. [42]	PS geometry, hip condition	Gait	HCF
	Bosmans et al. [43]	PS geometry, hip condition	Gait	Potentials of muscles to accelerate a joint
	Carriero et al. [44]	Hip condition	Gait	HCF, MF
	Choi et al. [45]	Multilevel surgery	Gait	Muscle lengths
	Scheys et al. [46]	PS geometry	Simulated hip range of motion	MMA
	Scheys et al. [47]	PS geometry	Gait	MMA
	Vandekerckhove et al. [48]	Simulated geometry & weakness	Gait	Hip moment generating capacities
	Wesseling et al. [49]	PS geometry	Gait	HCF, MF, MMA, muscle lines of action
Femoroacetabular impingement syndrome	Cannon et al. [50]	Cued gluteal activation	Squat	HCF
	Catelli et al. [51]	Osteochondroplasty, hip condition	Gait	HCF, MF
	Catelli et al. [3]	Osteochondroplasty, hip condition	Squat	HCF, MF
	Catelli et al. [52]	Osteochondroplasty, hip condition	Stairs	HCF, MF
	Ng et al. [53]	Hip condition, neck-shaft angle	Gait	HCF
	Ng et al. [54]	Hip condition	Gait	HCF, MF
	Samaan et al. [55]	Hip condition	Gait	MF
	Savage et al. [56]	Hip condition	Gait	HCF
	Tateuchi et al. [57]	Simulated muscle weakness	Squat	HCF, MF
Femoral version	Alexander et al. [58]	Hip condition	Gait	HCF, MF
	De Pieri et al. [59]	PS geometry	Gait	HCF, MF
	Modenese et al. [60]	Simulated femoral version	Gait	HCF
	Passmore et al. [61]	PS geometry, hip condition	Gait	HCF, MF

PS = patient-specific; THA = total hip arthroplasty; HJC = hip joint centre; MMA = muscle moment arms; HCF = hip contact forces; MF = muscle forces.

took the MSK model outputs and used them as inputs into different types of models (e.g., finite element models) to quantify acetabular cartilage and labrum stresses [53] and acetabular contact pressure or edge loading [32,50].

Each study was categorized in one of two ways: i) studies that compared different modeling and simulation methods in the context

Table 2
Overview of included studies' sample size (n) and demographics reported as means, medians, or ranges.

		Hip Disorder Group					Control Group				
Focus	Reference	n (M/F)	Age (y)	Mass (kg)	Height (m)	BMI (kg/m^2)	n (M/F)	Age (y)	Mass (kg)	Height (m)	BMI (kg/m^2)
Osteoarthritis	Bahl et al. [20]	10/5	68	NR	1.67	29	–	–	–	–	–
	Bahl et al. [5]	25/18	65	83	1.67	30	–	–	–	–	–
	Buehler et al. [21]	–	–	–	–	–	11/5	27	71	1.75	23
	Diamond et al. [22]	5/13	65	76	1.66	28	6/17	60	70	1.67	25
	Foucher et al. [23]	11/4	63	88	1.74	NR	9/6	56	73	1.71	NR
	Fuller and Winters [24]	0/9	50–70	NR	NR	NR	–	–	–	–	–
	Hoang et al. [25]	18*	64	77	1.66	28	–	–	–	–	–
	Lenaerts et al. [26]	15/5	52	NR	NR	NR	–	–	–	–	–
	Lenaerts et al. [27]	3/7	66	NR	NR	28	–	–	–	–	–
	Lenaerts et al. [28]	9/11	63	NR	NR	27	–	–	–	–	–
	Meyer et al. [29]	15/5	50	NR	1.73	26	9/8	53	NR	1.71	24
	Wesseling et al. [30]	5*	54	81	1.77	25	4*	56	63	1.68	22
	Wesseling et al. [31]	9/5	47	76	1.73	25	9/9	53	69	1.71	24
	Wesseling et al. [32]	–	–	–	–	–	1/1	26	74	1.79	23
	Van Rossom et al. [33]	12/9	63	75	1.75	NR	6/6	60	74	1.70	NR
Hip dysplasia	Delp et al. [34]	3*	NR	NR	NR	NR	–	–	–	–	–
	Gaffney et al. [35]	0/2	24	NR	NR	22	–	–	–	–	–
	Gaffney et al. [6]	0/4	25	NR	NR	24	–	–	–	–	–
	Harris et al. [36]	3/7	26	65	1.69	23	3/7	26	71	1.72	23
	Song et al. [13]	3/6	26	NR	NR	23	3/6	26	NR	NR	24
	Song et al. [37,38]	0/15	27	63	1.66	23	0/15	25	62	1.67	22
	Song et al. [4]	0/10	26	64	1.66	23	0/10	26	61	1.66	22
	Shepherd et al. [39]	0/14	27	NR	NR	23	–	–	–	–	–
	Shepherd et al. [40]	9*	22	NR	NR	23	9*	22	NR	NR	22
	Wu et al. [41]	0/20	21	62	1.70	23	0/15	23	65	1.70	22
Cerebral palsy	Bosmans et al. [42,43]	5/2	10	31	1.40	16	0/1	9	30	1.44	NR
	Carriero et al. [44]	3*	6–12	NR	NR	NR	10*	6–12	NR	NR	NR
	Choi et al. [45]	15/9	7	NR	NR	NR	17/11	8	NR	NR	NR
	Scheys et al. [46]	4/2	7–12	NR	NR	NR	–	–	–	–	–
	Scheys et al. [47]	5/2	10	31	1.39	16	–	–	–	–	–
	Vandekerckhove et al. [48]	3/2	7	21	1.19	14	0/1	9	30	1.39	NR
	Wesseling et al. [49]	5/2	10	31	1.39	16	–	–	–	–	–
FAIS	Cannon et al. [50]	4/4	30	78	1.74	NR	–	–	–	–	–
	Catelli et al. [51]	11/0	34	80	1.77	25	11/0	34	NR	1.75	25
	Catelli et al. [3]	10/0	35	NR	NR	26	10/0	34	NR	NR	26
	Catelli et al. [52]	10/0	33	NR	NR	25	10/0	32	NR	NR	25
	Ng et al. [53]	4/0	33	NR	NR	26	2/0	31	NR	NR	28
	Ng et al. [54]	18/0	38	NR	1.76	27	18/0	32	NR	1.76	26
	Samaan et al. [55]	14/10	36	NR	NR	25	14/10	42	NR	NR	24
	Savage et al. [56]	26/15	32	75	1.80	24	12/12	32	67	1.70	22
	Tateuchi et al. [57]	–	–	–	–	–	5/5	25	61	1.67	22
Femoral version	Alexander et al. [58]	16/26	13	45	1.56	NR	4/5	12	42	1.53	NR
	De Pieri et al. [59]	–	–	–	–	–	22/15	28	NR	NR	23
	Modenese et al. [60]	–	–	–	–	–	1/0	86	75	NR	NR
	Passmore et al. [61]	2/10	14	54	1.59	21	NR	14	52	1.56	NR

FAIS = femoroacetabular impingement syndrome; M = male; F = female; BMI = body mass index; NR = not reported. *Sex not reported.

of a hip disorder (n = 16) (e.g., compared generic versus patient-specific geometry) which will be referred to as "methods studies" (Table 3); or ii) studies that applied a single modeling workflow to study a hip disorder (n = 31) which will be referred to as "application studies" (Table 4).

3.2. Generic model development

Generic baseline models developed for the OpenSim or AnyBody software were used in 45 of the 47 studies (Tables 3 and 4). The remaining two studies used a custom algorithm [24] and an electromyography (EMG)-driven model programmed in MATLAB [50]. The OpenSim Gait2392 model was most commonly used (n = 26, Tables 3 and 4). Twenty of these studies indicated they used a version

Table 3
Summary of studies that compared modeling and simulation methods.

Reference	Comparisons	Additional Modeling Choices	Summary of Results and Conclusions
Bahl et al. [20]	Four models: 1) Shape modeling, PC fit 2) Shape modeling, CT 3) SMS with functional HJC 4) SMS with regression HJC	*Model:* Gait2392 (Models 3 & 4) *HJC:* CT-derived (Models 1 & 2) *MTU:* Re-mapped generic MTU (Models 1 & 2)	*Results:* Mean HJC location error for statistical shape models 1 and 2 (11.4 mm, 6.6 mm) were significantly lower than scaled generic models 3 and 4 (36.9 mm, 31.2 mm). Mean RMSE were greatest for hip MMA lengths using generic models (16.15–16.71 mm) versus shape models (0.05–3.2 mm). *Conclusion:* Shape modeling improves HJC location and MMA lengths.
Bosmans et al. [42]	Four model and gait conditions: 1)Generic, normal gait 2) Generic, CP gait 3) MRI, normal gait 4) MRI, CP gait	*Model:* Gait2392 Iteration (Details not reported) *Rigid Bodies:* SMS with global optimization *HJC:* MRI-derived (Models 3 & 4) *MTU:* MRI-based updated attachments & paths (Models 3 & 4) *Control:* SO	*Results:* Using MRI models, CP gait patterns reduced HCFs and changed the orientation of the HCF vector more vertically and anteriorly compared to normal gait. More pronounced bony deformities were correlated with greater differences in HCF magnitude and orientations. Using generic models, the HCFs during CP gait were more similar to those shown during normal gait. *Conclusion:* Femoral geometry influences HCFs.
Bosmans et al. [43]	Three model and gait conditions: 1)Generic, CP gait 2) MRI, CP gait 3) MRI, normal gait	*Model:* Gait2392 Iteration (Details not reported) *Rigid Bodies:* SMS with global optimization *HJC:* MRI-derived (Models 2 & 3) *MTU:* MRI-based updated attachments & paths (Models 2 & 3)	*Results:* The differences in muscles' potential to control joints between generic and MRI models were 398–894 ($^\circ/s^2$)/kg m, and 199–993 ($^\circ/s^2$)/kg m between gait conditions. MMA length changes were related to changes in potentials. *Conclusion:* CP gait and femoral deformities have a concomitant effect on muscle control hip and knee motion, mainly in the sagittal plane.
De Pieri et al. [59]	Two models: 1) Generic 2) Generic deformed to PS femoral version	*Model:* TLEM2 *Rigid Bodies:* SMS, radiograph-derived pelvic width scale factor *Control:* Inverse dynamics	*Results:* There were significant differences in the HCFs between models across the complete gait cycle including more anteriorly directed forces. HCFs during mid to terminal stance were less proximally and medially directed. *Conclusions:* PS femoral version may provide insight into joint damage risk.
Hoang et al. [25]	Two control models: 1)SO 2) EMG-assisted	*Model:* Gait2392 *Rigid Bodies:* SMS *HJC:* Regression *MTU:* Optimized muscle fiber & tendon slack length	*Results:* Compared to SO, EMG-assisted model had better agreement with EMG (i.e., higher R^2 and lower RMSE) and higher levels of muscle co-contraction. EMG-assisted had higher HCFs than SO and *in vivo* HCFs. *Conclusion:* EMG-assisted model solution can predict physiologically-plausible HCFs in a population with higher levels of muscle co-contraction.
Lenaerts et al. [26]	1) Sensitivity analysis of isolated changes in NL (40–80 mm) and NSA (110–150°) 2) Generic vs. deformed models (PS: NL & NSA)	*Model:* Gait2392 Iteration (7 segments, 16 DoF, 86 MTU) *Rigid Bodies:* SMS *Control:* SO	*Results:* Increasing NL increased the resultant HCF from 1.06 to 4.47 BW. NL predicted changes in all HCFs components' magnitudes and orientations in the frontal and sagittal planes. Increasing NSA increased gluteus medius and minimus activity. Increasing NL decreased gluteus medius activity. *Conclusion:* NL alters HCFs, NSA only has minor effect on HCF.
Lenaerts et al. [27]	Three models: 1) Generic 2) Generic deformed to PS femoral version, NL, & NSA 3) CT-derived pelvis	*Model:* Gait2392 Iteration (7 segments, 16 DoF, 86 MTU) *Rigid Bodies:* SMS with global optimization *HJC:* CT-derived (Model 3) *Control:* SO	*Results:* Model 3 with CT-derived geometry and HJC location, shifted the HJC on average 30.3 mm anteriorly and 20.9 mm proximally. Model 3 had significantly lower mean peak hip flexion-extension moment compared to the generic Model 1 (0.415 vs. 0.704 Nm/kg) and increased mean frontal plane HCF inclination angle (32.59°) compared to Model 1 (16.35°) and 2 (16.05°). *Conclusion:* Personalized geometry and HJC location affect HCFs.
Modenese et al. [60]	Generic model deformed with femoral version between -2° to 40°	*Model:* Full Body *Rigid Bodies:* Upper limbs removed, SMS *MTU:* Attachments & paths deformed *Control:* SO	*Results:* HCFs increased up to 17.9 % with increasing femoral anteversion. *Conclusion:* Femoral version substantially effects HCFs.

(*continued on next page*)

Table 3 (*continued*)

Reference	Comparisons	Additional Modeling Choices	Summary of Results and Conclusions
Passmore et al. [61]	Two models: 1) Generic 2) PS femoral version, NSA, & tibial torsion	*Model:* Gait2392 *Rigid Bodies:* SMS *HJC:* Radiograph-derived for patients *MTU:* Attachments & paths deformed (Model 2) *Control:* SO	*Results:* There were significant differences between models for hip muscle forces (RMSE = 0.05–0.18), and for HCFs (RMSE = 0.32–0.54). *Conclusion:* Torsional deformities increase hip abductor force, with a corresponding increase in compressive HCFs.
Scheys et al. [46]	Two models: 1) Generic 2) MRI-derived geometry	*Model:* Gait2392 Iteration (7 segments, 16 DoF, 86 MTU) *Rigid Bodies:* SMS with global optimization *HJC:* MRI-derived (Model 2) *MTU:* MRI-based updated attachments (Model 2)	*Results:* The mean difference in MMA lengths between models for hip sagittal, formal, and transverse plane muscles were 12.5 %, 30.1 %, and −96.5 %. *Conclusion:* Compared to MRI models, generic models overestimate MMA lengths for hip flexion, extension, abduction, adduction, and external rotation, and underestimate for hip internal rotation.
Scheys et al. [47]	Three models: 1) Generic 2) Generic deformed to PS femoral version, NL, & NSA 3) MRI-derived geometry	*Model:* Gait2392 Iteration (Details not reported) *Rigid Bodies:* SMS with global optimization *HJC:* MRI-derived (Model 3) *MTU:* Attachments & paths (Model 2), MRI-based updated attachments & paths (Model 3)	*Results:* Compared to the MRI model, the generic model on average overestimated the MMA lengths of the hip flexors (19.9 %), extensors (24.7 %), abductors (24.4 %), and adductors (8.0 %). Compared to the generic model, the deformed model only notably affected the MMA lengths for gluteus maximus. *Conclusion:* Large differences in MMA lengths were shown between the generic and MRI models, which were not uniformly reduced by the deformed model.
Shepherd et al. [39]	Deformed models of hip dysplasia patients with femoral version angles between −5° and 35°	*Model:* LaiArnold2017 Iteration (22 segments, 37 DoF, 92 MTU) *Rigid Bodies:* SMS, MRI-derived pelvis/femurs *HJC:* MRI-derived *MTU:* MRI-based updated attachments & paths *Control:* computed muscle control	*Results:* Increasing femoral anteversion resulted in the highest change of mean resultant HCFs in late stance (0.48 BW) and increased hip flexor and abductor muscle forces. HCFs were lowered by 0.32 BW on average with relative retroversion in late stance. *Conclusions:* Increased anteversion is the strongest influence on HCFs.
Song et al. [13]	Three models: 1) Generic 2) Generic with three CT-derived pelvis scale factors 3) CT-derived geometry	*Model:* 2396Hip *Rigid Bodies:* SMS (one scale factor per segment) *HJC:* CT-derived *MTU:* MRI-based updated attachments & paths *Control:* SO	*Results:* Mean resultant HCFs were significantly higher for CT-derived pelvis geometry (5.47 BW) versus the generic Model 1 (4.18 BW) and Model 2 (4.15 BW). The CT model showed significantly higher muscle forces compared to the generic models for hip flexors, extensors, internal rotators, and external rotators. *Conclusions:* Geometry, HJC, and muscle paths affect HCFs and muscle forces.
Vandekerckhove et al. [48]	6400 models with simulated hip muscle weakness (0–75 %), femoral version (20-60°) & NSA (120-160°). Simulated normal & CP gait patterns.	*Model:* Gait2392 Iteration (14 segments, 19 DoF, 88 MTU) *MTU:* MIMF scaled to participants' mass *Control:* SO	The capability gap (CG) in hip moment generating capacity increased by: 0.005–0.080 Nm/kg per 10 % hip abductor weakness increase; 0.011–0.211 Nm/kg per 10° femoral anteversion increase; and with 0.011–0.163 Nm/kg per 10° NSA increase. *Conclusion:* Increases in hip abductor weakness, femoral anteversion, and NSA predicted decreases in hip moment generating capacity at the hip.
Wesseling et al. [30]	Two MIMF scaling methods: 1) static: dynamometer 2) functional: strength required to generate joint moments during movements	*Model:* Gait2392 Iteration (14 segments, 19 DoF, 88 MTU) *Rigid Bodies:* SMS, MRI-derived geometry *HJC*: based on femoral bone structures *MTU:* MRI-based updated attachments & paths *Control:* SO	*Results:* Functional scale factors were higher than the static for abductors (median = 1.10 vs. 0.54) and flexors (0.94 vs. 0.41). Statically scaled models lacked sufficient strength to generate joint moments required for the movements. HCFs were similar between functionally scaled and unscaled models. *Conclusion:* Scaling model muscle forces is not required when quantifying HCFs if model is sufficiently strong.
Wesseling et al. [49]	Three models: 1) Generic 2) Deformed pelvis, femurs, & proximal tibia 3) MRI-derived pelvis, femurs, & tibias	*Model:* Gait2392 Iteration (14 segments, 19 DoF, 88 MTU) *Rigid Bodies:* SMS *HJC:* MRI-derived *MTU:* Attachments & paths deformed (Model 2), MRI-based	*Results:* There were higher differences between the generic and MRI model than between the deformed and MRI model for muscle position (2.19 vs. 1.73 cm), MMA length (3.34 vs. 2.13 cm), and muscle forces (6.53 vs. 3.08 N/kg). The generic model had lower peak HCFs than the MRI model (3.15 vs. 4.99 BW).

(*continued on next page*)

Table 3 (*continued*)

Reference	Comparisons	Additional Modeling Choices	Summary of Results and Conclusions
		updated attachments (Model 3) *Control:* SO	*Conclusion:* The deformed model is more similar to the MRI model than the generic but cannot yet serve as a replacement for the MRI model.

PC = principal components; CT = computed tomography; SMS = surface marker scaling; HJC = hip joint centre; CP = cerebral palsy; MRI = magnetic resonance imaging; PS = patient-specific; SO = static optimization; EMG = electromyography; NL = neck length; NSA = neck-shaft angle; MIMF = maximum isometric muscle force; MTU = musculotendon units; DoF = degrees of freedom; RMSE = root mean squared error; MMA = muscle moment arms; HCF = hip contact force.

of the Gait2392 model or the original Lower Extremity Model developed by Delp et al. [62] adapted with different numbers of segments, musculotendon units, or degrees of freedom compared to the original models (Tables 3 and 4). Fifteen studies used a different OpenSim generic model and three used the generic Anybody Twente Lower Extremity Model Version 2 (TLEM2) [63] (Tables 3 and 4).

Thirty-three of the studies used generic models with geometry that was developed primarily using data from samples of one to five older adults and cadaveric specimens (i.e., Gait2392, 2396Hip, Full Body Running, TLEM2) [62–67]. In comparison, only 11 studies used one of the four generic models (i.e., Full Body, LaiArnold2017, 2398Hip, Full Body Squat) developed based on musculotendon parameters derived from MRIs of 24 young, healthy individuals (age range = 12–51) and 21 cadaveric specimens [12,68]. Furthermore, the 2396Hip and 2398Hip models, which include additional muscles and updated muscle parameters to be more suitable for hip research, were only used in seven studies.

The most common muscle model and method to estimate muscle activations and forces was OpenSim's static optimization (n = 29, Tables 3 and 4) which uses a Hill-type muscle model in series with a stiff tendon that neglects passive muscle force contributions [69, 25]. In addition, four studies used computed muscle control and three used EMG-assisted models in OpenSim (Tables 3 and 4). AnyBody's inverse dynamics-based approach, that uses a third-order polynomial recruitment criteria, was used in three studies (Tables 3 and 4) [19]. The passive musculotendon force contributions are accounted for in the computed muscle control [69], EMG-assisted [70], and inverse dynamics-based approaches [63].

3.3. Model validation

Only eleven (27 %) studies included in this review performed model validations (Table 5). The validations were primarily qualitative, and no studies reported any quantitative validation metrics or statistics to quantify the agreement between modeled and experimental HCFs or hip muscle activations (Table 5). Validation for models of more than one patient with a structural hip disorder occurred only within studies examining patient-specific models of people with hip dysplasia and osteoarthritis (Table 5). Thus, no studies validated generic models for structural hip disorder patients in a sample size greater than one. Furthermore, only seven studies reported that kinematic tracking errors, residual forces, and residual moments were within the recommended limits to verify model quality (Table 5).

Fig. 2 provides an overview of the original and subsequently developed generic OpenSim models and validations, which we were able to retrieve from the references in the included studies and the software's documentation. These models were also validated using primarily qualitative methods and with samples of one to ten healthy controls (Fig. 2). The most common experimental data used was muscle activations from young, healthy adults and cadaveric muscle moment arm data from older adults [12,62,64,65,71–73].

3.4. Methods studies

Sixteen studies compared different modeling and simulation methods in the context of structural hip disorders (Table 3). Four of these studies also included analysis of the effect of hip conditions (e.g., patients versus healthy controls) (Table 1). Eleven studies compared the level of model rigid body geometry personalization. In general, there were three levels of model personalization: i) generic models (i.e., geometry scaled based on measures of surface marker locations); ii) deformed models (i.e., scaled generic models deformed to match with imaging measures of patients' femoral version angle, neck-shaft angle, and/or neck length); and iii) image-derived models (i.e., scaled generic models with rigid bodies replaced by fully patient-specific three-dimensional (3D) geometries derived from magnetic resonance imaging (MRI) or computed tomography (CT) scans) (Table 3). A subset of these model geometry personalization studies investigated statistical shape modeling (n = 1) and hip joint center (HJC) estimation methods (n = 1) (Table 3). Four studies also performed sensitivity analyses to determine the effect of modeling different femoral version angles (n = 3), femoral neck-shaft angles (n = 2), muscle weakness (n = 2), and femoral neck length (n = 1) (Table 3). Overall, studies showed that incorporating fully patient-specific 3D pelvis and femur geometries and image-based HJCs resulted in different muscle moment arms, muscle forces, and HCFs than those quantified using generic models (Table 3). There were conflicting results regarding whether deforming generic model geometry to match individuals' measurements (e.g., angle) is an appropriate method to improve model accuracy while minimizing computational cost (Table 3).

The effect of different approaches for estimating muscle activations and the use of muscle strength scaling on model outputs were also investigated. For example, one study demonstrated that EMG-informed modeling improved the estimation of muscle co-contraction in osteoarthritis patients compared to static optimization (Table 3). In addition, one study examined the effect of two methods to scale the model's maximum isometric muscle forces, which showed that there was either no effect on the HCFs or the model

Table 4
Modeling choices for the included studies that applied a generic model to answer a research question.

Model	Reference	Rigid Bodies	HJC	Musculotendon Units	Control
Lower Extremity Model (7 segments, 7 DoF, 43 MTU)	Delp et al. [34]	NR	NR	NR	N/A
Gait2392 (14 segments, 23 DoF, 92 MTU)	Bahl et al. [5]	Statistical shape modeling	CT-derived	NR	SO
	Buehler et al. [21]	SMS	Regression	MIMF scaled to participants' mass	SO
	Diamond et al. [22]	SMS	NR	Optimized muscle fiber/tendon slack length	EMG-assisted
	Ng et al. [54]	SMS, CT-derived pelvis scale factors	NR	MIMF scaled to mass & height	SO
Gait2392 (14 segments, 19 DoF, 88 MTU)	Meyer et al. [29]	SMS	NR	NR	SO
	Wesseling et al. [31]	SMS	NR	Muscle attachments, fiber/tendon slack lengths scaled with rigid body scale factors	SO
Gait2392 (7 segments, 16 DoF, 86 MTU)	Carriero et al. [44]	SMS	NR	NR	SO
	Lenaerts et al. [28]	SMS	NR	NR	SO
Gait2392 (8 segments, 19 DoF, 92 MTU)	Samaan et al. [55]	SMS	NR	NR	CMC
Gait2392 (3 DoF knee)	Van Rossom et al. [33]	SMS	NR	NR	SO
Gait2392 (34 MTU)	Savage et al. [56]	SMS	Regression	Optimized muscle fiber/tendon slack length MIMF scaled to mass & height	EMG-assisted
Gait2392 (version not specified)	Choi et al. [45]	NR	NR	NR	N/A
	Foucher et al. [23]	NR	NR	NR	Constraints
	Wesseling et al. [32]	SMS, MRI-derived pelvis, femurs, tibias, & patellae	MRI-derived	Hip & knee muscle attachments updated based on MRI & bony landmarks	SO
Full Body Running (12 segments, 29 DoF, 92 MTU)	Ng et al. [53]	NR	NR	NR	SO
Fully Body (22 segments, 37 DoF, 80 MTU, 17 ITA)	Catelli et al. [51]	SMS, 10x weighting for markers verified with CT	NR	NR	SO
LaiArnold2017 (22 segments, 37 DoF, 80 MTU, 17 ITA)	Gaffney et al. [35]	SMS, MRI-derived pelvis & femurs	MRI-derived	Hip & knee muscle attachments updated based on MRI & bony landmarks	SO
Full Body Squat (22 segments, 37 DoF, 80 MTU, 17 ITA)	Catelli et al. [3,52]	SMS, 10x weight CT verified markers verified with CT	NR	NR	SO
	Gaffney et al. [6]	SMS, MRI-derived pelvis & femurs	MRI-derived	Hip & knee muscle attachments updated based on MRI, MIMF scaled to torque data	CMC
2396Hip (14 segments, 23 DoF, 96 MTU)	Harris et al. [36]	SMS, CT-derived pelvis	CT-derived	Hip muscle attachments & paths updated based on MRI & bony landmarks	SO
	Shepherd et al. [40]	SMS, MRI-derived pelvis & femurs	MRI-derived	Hip muscle attachments & paths updated based on MRI & bony landmarks	CMC
2398Hip (14 segments, 23 DoF, 98 MTU)	Song et al. [4,37,38]; Wu et al. [41]	SMS, MRI-derived pelvis & femurs	MRI-derived	Hip muscle attachments & paths updated based on MRI & bony landmarks	SO
TLEM2 (11 segments, 21 DoF, 110 MTU)	Alexander et al. [58]	SMS, personalized femoral version	NR	NR	Inverse dynamics
	Tateuchi et al. [57]	SMS	NR	Simulated hip muscle weakness	Inverse dynamics
Custom Models	Fuller and Winters [24]	NR	NR	NR	Heuristic
	Cannon et al. [50]	NR	NR	NR	EMG-driven

DoF = degrees of freedom; MTU = musculotendon units; ITA = ideal torque actuators; NR = not reported; SMS = surface marker scaling; CT = computed tomography; MRI = magnetic resonance imaging; HJC = hip joint centre; MIMF = maximum isometric muscle force; SO = static optimization; CMC = computed muscle control.

lacked sufficient strength required to generate the joint moments observed during the dynamic tasks (Table 3).

3.5. Application studies

Thirty-one studies applied a single modeling workflow to answer a research question related to a structural hip disorder (Table 4). Fourteen studies used the models to compare outputs between hip conditions, four studies compared pre- and post-treatment outputs

Table 5
Summary of model validations performed in the included studies.

Reference	Model	Results Summary
Buehler et al. [21]	*Baseline:* Gait2392 *Sample:* 16 controls *Patient-specific:* no	*Quantitative:* NR *Qualitative:* "The shape and maximum values of the Orthoload waveforms were similar to the waveforms obtained from our participants, with exception of the [HCF] of the movement leg for the hip abduction exercise, which showed higher values in our participants." "[HCF] from all exercises in this study showed a reasonable agreement with the values from OrthoLoad."
Lenaerts et al. [26]	*Baseline:* Gait2392 Iteration *Sample:* 1 OA patient *Patient-specific:* no	*Quantitative:* NR *Qualitative:* Figures comparing EMG and modeled muscle activity across gait cycle
Lenaerts et al. [27]	*Baseline:* Gait2392 Iteration *Sample:* 10 OA patients *Patient-specific:* yes	*Quantitative:* Compared to OrthoLoad *in vivo* HCFs, the modeled HCFs had higher magnitudes (3.43 vs. 2.38 BW) and frontal plane inclination angles (33° vs. 13°) *Qualitative:* "The presence of pathological hip kinematics … contributes to the observed differences [in HCFs]"
Gaffney et al. [35]	*Baseline:* LaiArnold2017 *Sample:* 2 HD patients *Patient-specific:* yes	*Quantitative:* RF < 10 N for most of gait cycle, max anterior and superior RF < 25 N, max medial RF > 25 N, RM < 50 Nm *Qualitative:* Agreement was shown between modeled and experimental muscle activations, and with the HCFs of the previous modeling study
Gaffney et al. [6]	*Baseline:* Full Body Squat *Sample:* 4 HD patients *Patient-specific:* yes	*Quantitative:* RF: anterior = 21.3 (10.2) N; superior = 23.5 (8.3) N; lateral = 29.5 (19.2) N *Qualitative:* "Model estimated activation timing qualitatively agreed with experimentally collected [EMG]"
Harris et al. [36]	*Baseline:* 2396Hip *Sample:* 1 control *Patient-specific:* yes	*Quantitative:* RF < 0.05 BW, RM < 0.3 Nm/kg *Qualitative:* "Model-based activations qualitatively agreed with EMG signals" "… hip JRFs for controls fell near the upper range of those measured in-vivo with telemeterized implants … and previous models …" Kinematics, joint moments, and muscle forces were comparable to previous studies
Modenese et al. [60]	*Baseline:* Full Body *Sample:* 1 control *Patient-specific:* yes	*Quantitative:* Reported peak errors, root mean squared errors, and coefficients of determination for comparisons between modeled and experimentally measured knee contact forces (most accurate models were 5° and 12° of femoral anteversion) *Qualitative:* NR
Samaan et al. [55]	*Baseline:* Gait2392 Iteration *Sample:* 1 (FAIS patient or control) *Patient-specific:* no	*Quantitative:* Root mean squared errors: pelvic translations <1.1 cm; pelvic rotations <0.60°; angles <1.45°; RF <0.66 %BW; RM <0.52 %BW*Height *Qualitative:* "A good qualitative match was found between the EMG and [computed muscle control] estimated muscle activations"
Shepherd et al. [39]	*Baseline:* LaiArnold2017 *Sample:* 14 HD patients *Patient-specific:* yes	*Quantitative:* NR *Qualitative:* "… residual forces and moments were minimized to recommended levels …" "Muscle activation timing during gait was checked for qualitative agreement with surface EMG signals …"
Shepherd et al. [40]	*Baseline:* 2396Hip *Sample:* NR *Patient-specific:* yes	*Quantitative:* NR *Qualitative:* "… minimizing residual forces and moments as well as comparing surface electromyography data to predicted muscle activations based on ON/OFF timing and root mean square errors …"
Song et al. [37]	*Baseline:* 2398Hip *Sample:* 15 HD patients, 15 controls *Patient-specific:* yes	*Quantitative:* Tracking errors = <2 cm; RF < 0.025 BW; RM < 0.4 Nm/kg *Qualitative:* "Model-estimated muscle activation qualitatively agreed with EMG timings." "Hip muscle forces and JRFs were in ranges similar to recent subject-specific modeling studies"

NR = not reported; OA = osteoarthritis; HD = hip dysplasia; FAIS = femoroacetabular impingement syndrome; HCF = hip contact force; EMG = electromyography; BW = body weight; RF = residual forces; RM = residual moments; JRF = joint reaction force.

in patients (e.g., surgical treatment or cued gluteal muscle activation), and five evaluated both a hip condition and a treatment (Table 1). In addition, four studies modified the models to simulate surgical treatment or rehabilitation. Three studies collected data from healthy controls only to investigate a variable related to a structural hip disorder (e.g., HCFs during hip-focused rehabilitation exercises or the effect of muscle weakness on HCFs) (Table 1). Lastly, one study evaluated osteoarthritis patients only to determine the HCFs in response to different rehabilitation exercises (Table 1).

Table 4 summarizes the modeling parameters for application studies that used a baseline generic model. The rigid body geometry of generic models was most commonly modified to represent an individual using surface marker-based scaling with (n = 14) or without (n = 10) additional personalization from medical imaging. In addition, one study used statistical shape modeling. However, four studies did not report how the models' rigid bodies were scaled or personalized to represent individual participants. Of the studies that only used surface marker-based scaling, two reported adjusting the HJCs using regression equations. Of the studies that incorporated medical imaging to create patient-specific models, nine implemented image-derived pelvis 3D geometries, eight of which also included femurs. In addition, patient-specific HJCs were typically determined by a least-squares approach to establish the centre of a sphere fit to either the acetabulum or the head of the femur. The remaining studies used imaging data to verify weightings of pelvis markers (n = 3), create pelvis scale factors (n = 1), or deform the generic femur geometry to match the patient-specific femoral version angle (n = 1).

Musculotendon units were also personalized in thirteen application studies (Table 4). For studies that did not replace the generic model geometry, the maximum isometric muscle forces were scaled to the participants' mass and/or height (n = 3), and the muscle fiber and tendon slack lengths were optimized (n = 2). When image-derived 3D geometries were used to create patient-specific models, the MRIs and knowledge of bony landmarks indicating muscle origin and insertion locations were used to update the muscle paths and attachments. Only one study that used patient-specific models scaled the baseline generic models' maximum isometric muscle forces to experimental torque data.

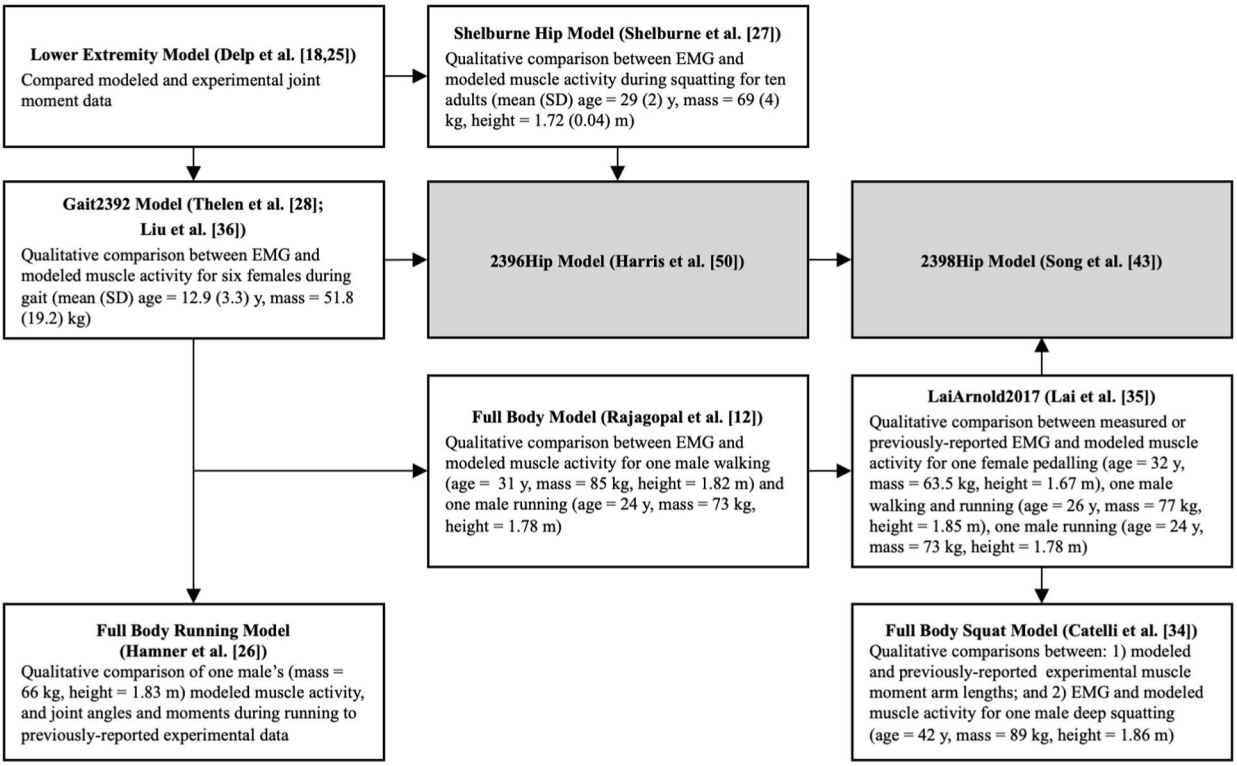

Fig. 2. Overview of sequentially developed generic OpenSim models commonly used in the included studies of structural hip disorders showing validations of the original and subsequent model iterations indicated by arrows. EMG = electromyography; y = years. Grey boxes indicate models described in studies included in this review (Table 5).

3.6. Experimental data

Most of the studies collected experimental data which served as model inputs to simulate movement. Motion capture data was collected with various optical tracking systems (n = 46), and ground reaction forces were measured with either force plates (n = 37) or instrumented treadmills (n = 6), (Table 6). Table 6 shows the wide variability in kinematic and kinetic data collection methods across studies. In addition, there was a notable lack of reporting of data collection and signal processing techniques (Table 6). For example, seven studies reported using a 70-marker set (Table 6); however, we could not retrieve information about marker locations from any of these studies or references. Multiple studies did not report the sampling rate for kinematic (n = 11) and kinetic data (n = 10) or how they filtered kinematic (n = 22) and kinetic (n = 19) data. The 11 studies that collected EMG data also demonstrated variability in the signal processing techniques (Table 7). Furthermore, more than a third of EMG studies did not include information on how the EMG signals were filtered (n = 3) or normalized (n = 2).

4. Discussion

Forty-seven studies were identified in this scoping review that used MSK models as a tool to research structural hip disorders. The hip disorders investigated in these studies included osteoarthritis, hip dysplasia, cerebral palsy-associated femoral deformities, FAIS, and idiopathic femoral version deformities. The models were primarily used to quantify HCFs and muscle forces or activations in response to dynamic tasks *in vivo*. Generic OpenSim models were most commonly used. However, there were a lack of quantitative methods used to validate these generic models, especially in the context of structural hip disorders. In addition, the use of recommended methods from studies that compared various modeling and simulation techniques was limited in studies that used the models to answer clinical research questions. Lastly, the wide variability and under-reporting of data collection, data processing, and modeling methods present barriers to comparing studies and limit study reproducibility.

4.1. Model development and validation

Retrieving information regarding model development and validation results for the generic models presented a challenge due to missing detailed descriptions of models and model iteration information that was common in structural hip disorder modeling studies. Based on our knowledge, the common generic models reported in the included studies were primarily developed based on data from

Table 6
Kinematic and kinetic instrumentation and signal processing information for the included studies.

	Kinematics					Kinetics			
Reference	Cameras	Marker Set	SR (Hz)	Filter	FC (Hz)	Force Plates	SR (Hz)	Filter	FC (Hz)
Alexander et al. [58]	NR	Plug-in gait	200	2nd order LPB	5	NR	1000	2nd order LPB	12
Bahl et al. [5]	10	12 markers + 4 rigid clusters	100	NR	NR	–	–	–	–
Bahl et al. [20]	10	6 DoF	100	2nd order LPB	6	2	2000	2nd order LPB	10
Bosmans et al. [42]	8	SIMM	100	NR	NR	2	1500	NR	NR
Bosmans et al. [43]	8	SIMM	100	NR	NR	2	1500	NR	NR
Buehler et al. [21]	12	21 markers + 5 rigid clusters	100	NR	NR	2	1000	NR	NR
Cannon et al. [50]	11	24 markers + 6 rigid clusters	250	2nd order LPB	6	2	1500	2nd order LPB	12
Carriero et al. [44]	7	Helen-Hayes	50	NR	NR	2	NR	NR	NR
Catelli et al. [51]	10	3UOMAM	200	4th order LPB	6	2	1000	4th order LPB	6
Catelli et al. [3]	10	UOMAM	200	4th order LPB	6	2	1000	4th order LPB	6
Catelli et al. [52]	10	Modified Plug-in gait	200	4th order LPB	6	3	1000	4th order LPB	6
Choi et al. [45]	7	NR	NR	NR	NR	2	NR	NR	NR
De Pieri et al. [59]	13	Institute for Biomechanics	200	4th order LPB	10	3	1000	4th order LPB	20
Diamond et al. [22]	12	51 markers	200	2nd order LPB	6	2	1000	2nd order LPB	6
Foucher et al. [23]	4	6 markers	NR	NR	NR	1	NR	NR	NR
Fuller and Winters [24]	NR	14 markers	NR	NR	NR	2	NR	NR	NR
Gaffney et al. [35]	NR	70 markers	100	4th order LPB	8	Treadmill	2000	4th order LPB	30
Gaffney et al. [6]	10	70 markers	100	4th order LPB	8	NR	2000	4th order LPB	20
Harris et al. [36]	10	Modified Helen-Hayes	100	LPB	6	4	1000	LPB	20
Hoang et al. [25]	12	51 markers	200	2nd order LPB	6	2	1000	2nd order LPB	6
Lenaerts et al. [26]	NR	NR	NR	NR	NR	NR	NR	NR	NR
Lenaerts et al. [27]	8	Plug-in gait	NR	NR	NR	2	NR	NR	NR
Lenaerts et al. [28]	6	Plug-in gait	NR	NR	NR	2	NR	NR	NR
Meyer et al. [29]	15	Plug-in gait	100	WF*	–	2	1500	2nd order LPB	6
Modenese et al. [60]	NR	NR	NR	NR	NR	NR	NR	NR	NR
Ng et al. [53]	10	UOMAM	NR	WF*	–	2	NR	4th order LPB	6
Ng et al. [54]	10	UOMAM	200	4th order LPB	6	2	1000	4th order LPB	6
Passmore et al. [61]	10	Plug-in gait	100	WF*	–	NR	1000	WF*	–
Samaan et al. [55]	10	29 markers + 4 rigid clusters	250	4th order LPB	6	2	1000	4th order LPB	50
Savage et al. [56]	12	GUFBMS	120 or 100	2nd order LPB	6	2	1200 or 1000	2nd order LPB	6
Scheys et al. [46]	8	SIMM	NR	NR	NR	–	–	–	–
Scheys et al. [47]	8	SIMM	NR	NR	NR	–	–	–	–
Shepherd et al. [39]	10	70 markers	100	4th order LPB	8	Treadmill	2000	4th order LPB	6
Shepherd et al. [40]	10	70 markers	100	NR	NR	Treadmill	2000	NR	NR
Song et al. [13]	NR	Modified Helen-Hayes	100	4th order LPB	6	NR	1000	4th order LPB	20
Song et al. [37]	10	70 markers	100	4th order LPB	8	Treadmill	2000	4th order LPB	6
Song et al. [38]	10	70 markers	100	LPB	8	Treadmill	2000	LPB	6
Song et al. [4]	10	70 markers	100	LPB	8	2	2000	LPB	10
Tateuchi et al. [57]	8	Plug-in gait	100	4th order LPB	6	NR	1000	4th order LPB	6
Vandekerckhove et al. [48]	12	Plug-in gait	100	NR	NR	2	1000	NR	NR
Van Rossom et al. [33]	13	Modified Plug-in gait	100	NR	NR	NR	1000	NR	NR
Wesseling et al. [30]	NR	Plug-in gait	100	NR	NR	2	1500	NR	NR
Wesseling et al. [31]	NR	Plug-in gait	100	NR	NR	2	1500	NR	NR

(*continued on next page*)

Table 6 (*continued*)

	Kinematics					Kinetics			
Reference	Cameras	Marker Set	SR (Hz)	Filter	FC (Hz)	Force Plates	SR (Hz)	Filter	FC (Hz)
Wesseling et al. [49]	8	SIMM	100	NR	NR	2	1500	NR	NR
Wesseling et al. [32]	10	Plug-in gait	100	NR	NR	2	1000	NR	NR
Wu et al. [41]	NR	NR	NR	NR	NR	Treadmill	NR	NR	NR

NR = not reported; SR = sampling rate; FC = filter cut-off; LPB = low-pass Butterworth; WF = Woltring filter. *Mean squared error = 15 mm^2.

Table 7
Electromyography instrumentation and signal processing information for the included studies.

Reference	Muscles	SR (Hz)	CMMR (db)	BP Filter (Hz)	Rectification	Envelope	FC (Hz)	Normalization
Cannon et al. [50]	6	1500	NR	30–500	Full-wave	2nd order LPB filter	2.5	MVIC
Diamond et al. [22]	16	1000	NR	30–300	Full-wave	Low-pass filter	6	Max from gait, CMJ, and MVIC
Fuller and Winters [24]	8	NR	NR	NR	Full-wave	2nd order low-pass RC filter	2.88	MVIC
Gaffney et al. [35]	8	2000	>100	NR	NR	NR	NR	MVIC
Gaffney et al. [6]	8	NR	>100	NR	NR	NR	NR	NR
Hoang et al. [25]	16	1000	NR	30–300	Full-wave	Low-pass filter	6	Max from gait, CMJ, and MVIC
Lenaerts et al. [26]	8	1560	NR	12.5–62.5	NR	Root mean square	NR	Trial max
Passmore et al. [61]	10	1000	NR	10–400	Full-wave	Low-pass filter	6	NR
Samaan et al. [55]	12	2000	NR	20–500	Full-wave	4th order LPB filter	6	MVIC
Savage et al. [56]	14	1200 or 1000	NR	30–300	Full-wave	LPB	6	Max from gait, CMJ, and MVIC
Song et al. [37]	8	2000	NR	10–350	Full-wave	4th order LPB filter	10	Trial max

SR = sampling rate; CMMR = common mode rejection ratio; BP = bandpass, FC = filter cut-off; NR = not reported; LPB = low-pass Butterworth; RC = resistor-capacitor; MVIC = maximum voluntary isometric contraction; max = maximum; CMJ = counter-movement jump.

older adults and cadaveric specimens [63,62,66,73], then most commonly validated using experimental muscle activation data from young, healthy adults [12,64,65,71,72]. In contrast, the populations in the included studies demonstrated large heterogeneity in demographics and activity levels (Table 2). The validations performed in the included studies of structural hip disorders were also primarily limited to qualitative assessments of experimental and model data agreement. While validation guidelines have been shared in terms of the timing of muscle activations and agreement with experimental HCFs [2], these quantitative validation methods have not been widely adopted in the modeling of structural hip disorders. Therefore, additional validation is required to assess the representativeness of the generic models to quantify hip joint mechanics in the specific populations of interest. Ongoing validation of the models shared by researchers would generate important, up-to-date knowledge of the accuracy of current models.

Updated validation thresholds are needed that are specific to populations with structural hip disorders. For example, it is currently recommended that modeled HCFs fall within two standard deviations of experimental HCFs [2]. However, experimental HCFs are only available from instrumented hip prostheses in total hip arthroplasty (THA) patients [74,75]. Therefore, it is likely that previously-reported differences between the model and experimental HCFs are more attributable to the inherent demographic and physical differences between older THA patients and other populations (e.g., young active adults with FAIS) rather than the errors within the models themselves. Specifically, when young, healthy adults squat to maximum depth, their HCFs have been noted to reach values greater than two standard deviations higher than the older THA patients; however, when looking at the HCFs of the young adults when at the mean knee flexion angle of the THA patients (i.e., 71°), the HCFs are lower than the THA patients and within two standard deviations [76]. These findings suggest a need for continued discussions to determine the level of modeling validation required to answer clinically relevant research questions. It is also evident that more representative experimental data sets are required.

4.2. Modeling and simulation methods

Overall, the studies included in this review that compared generic and patient-specific modeling methods recommended using patient-specific models. This recommendation was based on their results demonstrating differences in HCFs and muscle moment arms between models with different levels of geometry personalization. However, due to the challenges of measuring *in vivo* HCFs for validation and a lack of validation studies quantitatively comparing experimental and modeled muscle activations and parameters, it is unclear whether the patient-specific models are truly more accurate. This likely contributes to the lack of adoption of patient-specific modeling in application studies, with only 36 % of studies using image-derived 3D geometries.

A potential concern with patient-specific modeling methods is that they rely on semi-manual adjustment of muscle paths to match

imaging data and anatomical descriptions of muscle attachments from the literature [6,47]. Thus, it is suggested that there is a potential for inter-operator and inter-patient errors when creating patient-specific models [77,78]; however, the amount of error in modeling of different structural hip disorders is unclear and not reported. In addition, since MRIs only capture static positions, there is uncertainty regarding the accuracy of MRI-based muscle paths through the entire joint range of motion [37]. Muscle moment arms and lines of action can be a significant source of error in model muscle activation and HCF estimations and may primarily account for differences in output between patient-specific and generic MSK models [49]. Given the cost of acquiring MRIs or CT scans for study participants and the time required to generate patient-specific models, it is important to determine the level of model geometry personalization and accuracy required to answer given research questions. Quantitative validations are also essential to help establish this threshold for accuracy.

The methods study conducted by Hoang et al. [25] established that EMG-informed models better predict muscle co-activation compared to static optimization; however, only two subsequent studies have used the EMG-informed approach [22,56]. Static optimization assumes that the neural control strategy in healthy individuals involves minimizing muscle co-activation [79] and thus may underestimate muscle activation in those with hip osteoarthritis given that they are expected to demonstrate increased co-activation [22]. EMG-informed models also consistently estimated significantly higher HCFs than static optimization across the gait cycle [25]. The increased HCFs are likely a result of increased co-activation caused by differences in neural control between the pathological and healthy populations [22], as well as passive muscle force contributions in the EMG-informed models which are neglected when using static optimization [25]. Given that most studies applying models to study a specific hip disorder are interested in the relative difference in HCFs between populations or time points, knowing the error between methods for estimating muscle forces can help to evaluate whether these modeling decisions would impact the overall interpretation of study results. Future comparisons between HCFs estimated with static optimization versus EMG-informed models in populations with other hip disorders with or without abnormal patterns of muscle co-contraction will help to support researchers' decisions about control models.

The current review also highlighted that MSK modeling of structural hip disorders is still predominately used to investigate tasks with limited hip range of motion (e.g., gait). Studies investigating young adult hip disorders, such as FAIS and hip dysplasia, were a notable proportion of the articles included in this review. Given that these populations are generally young and active, tasks such as gait may not be sufficient to comprehensively evaluate abnormal hip mechanics using MSK modeling. This divide may be present because modeling of the hip has primarily been focused on individuals with cerebral palsy or hip osteoarthritis, who typically present with more severe gait deficits than those shown in FAIS or hip dysplasia patients [22,29,36,42,51]. Models that simulate deep squats [71,72,37] have been recently developed but have yet to be widely adopted. In addition, the 2396Hip model was recently modified and quantitatively validated in healthy controls to simulate dynamic tasks with increased multiplanar hip joint ranges of motions [76]. Further development, validation, and application of models to investigate a wider variety of clinically relevant tasks is an important area of opportunity and advancement for MSK modeling of structural hip disorders.

4.3. Study reproducibility

The results of this scoping review highlight inconsistencies in the reporting of modeling and simulation method details. For example, it was common for studies using an iteration of the Gait2392 model to cite the original article describing the original Lower Extremity Model developed by Delp et al. [62] without specifying which iteration of the model they were utilising. This is challenging because the same citation was used in studies that had implemented models with different numbers of segments, musculotendon actuators, or degrees of freedom; thus, it was often unclear which model was being used in multiple studies. There was also minimal reporting of the details at other stages of the modeling and simulation workflow. For example, few studies clarified how many scale factors were used to scale the models and which markers were used to calculate the scale factors. In addition, only seven studies reported the residual errors for marker location for scaling or tracking during inverse kinematics and the residual forces or moments during inverse dynamics. More detailed reporting guidelines should be established and enforced to help researchers assess their modeling studies and improve reproducibility.

Reporting the instrumentation specifications and data collection and processing techniques was inconsistent across studies. For example, many studies did not report sufficient details of the marker set used, the number of cameras, or the sampling rate at which data was collected. Previous studies have shown that these data collection parameters can strongly influence the results of biomechanical analyses. Specifically in modeling, Mantovani and Lamontagne [80] demonstrated significant differences in joint angles calculated in OpenSim between three marker set configurations. Two of these configurations were commonly used in the studies included in this review (Plug-in-Gait and the University of Ottawa Motion Analysis Model). However, it remains unclear how different marker sets may influence other model outputs such as the commonly estimated HCFs. Studies have also shown variations in biomechanical outcomes between labs, specifically with joint moments when a standardized protocol is not being used [81,82]. Furthermore, the largest inter-laboratory inconsistency in gait measurements was pelvis anthropometric measures, which are critical to the most common marker-based scaling and HJC estimation methods used in the studies included in this review. Enhancing the clarity in the reporting of data collection and processing techniques will likely make it easier to assess the accuracy and reproducibility of the results.

It was unclear how the raw experimental data was processed in 48 % and 44 % of studies using kinematic and kinetic data, respectively. In addition, most of the studies that reported how the data was filtered did not describe the rationale behind choosing a specific filter cut-off frequency. Cut-off frequency choice is an important signal processing consideration, particularly when filtering data that will be input into MSK models. For example, Tomescu et al. [83] compared different marker and ground reaction force filter cut-off frequency conditions and quantified significant differences in model-predicted muscle forces, joint contact forces, and residual

forces and moments. A greater emphasis should be placed on reporting the signal processing details of input data for models as it can profoundly impact the results of modeling studies. While there are unavoidable uncertainties and assumptions required in MSK modeling, good and transparent data collection and processing methods can be easily implemented to help improve researchers' and clinicians' ability to interpret the clinical relevance of modeling simulation results.

5. Conclusion and future research

MSK models are a powerful tool to provide insight into factors that are typically not feasible to measure *in vivo*, such as HCFs and activations of the deep musculature. Furthermore, they represent an opportunity to simulate the effects of treatments and generate inputs for different scales of models, such as finite element models, to address broader research questions. This scoping review identified that there is limited quantitative data available to fully understand the accuracy of MSK models, specifically in the context of structural hip disorders. More stringent validation studies will also help researchers reach a consensus on the level of model personalization and appropriate methods for estimating muscle activations required for MSK models that are focused on structural hip disorders. Increased transparency in reporting data collection, signal processing, and modeling methods is needed to increase study reproducibility and allow researchers and clinicians to better assess modeling study results.

Based on this scoping review, we have several recommendations for future research related to modeling in structural hip disorder research. First, we created a template table that researchers can complete and include as a table within the methodology section of their manuscripts (Appendix C). This will encourage transparency by allowing researchers to report the important details related to reproducibility and methods evaluation, while avoiding the limitation of word count restrictions and maintaining the focus on the main research question for improved readability for general audiences.

Second, we recommend that studies using EMG to validate their models, implement a quantitative approach that involves statistical analysis between model and experimental muscle activations (e.g., cross-correlation, RMSE, Bland-Altman). In addition, a specific threshold for identifying the on and offset timing for muscle activations should be reported considering the wide variety of approaches available [84]. Other validation approaches used in the literature that could be applied to models for hip disorder research are the use of dynamic MRIs for joint kinematics and contact loading [85]. Furthermore, Uhlrich et al. [86] demonstrated how models can be assessed by evaluating the impact of muscle coordination re-training that was designed based on modeling insights.

Third, machine learning has the potential to improve the reliability and accuracy of modeling studies. For example, the reliability of kinematic input data can be improved using markerless motion capture (e.g., Theia3D) [87]. In addition, algorithms used to estimate kinematics from wearable sensors offer the advantage of affordable, easy to use, and portable data collection in environments outside the laboratory, such as the clinic, home, work, or sporting environments [88]. The ability to capture kinematics in individuals' natural environment may reflect more accurate movement patterns and facilitate long-term monitoring [88]. Machine learning could also be used to identify common muscle synergies in patients with pathologies, then train neural control models of muscle activation to create generic models of muscle coordination for specific pathologies [89]. Lastly, automated approaches to create personalized muscle paths in models based on MRIs could be applied to increase the reliability of muscle paths [77].

Ethical approval statement

The ethical statement is not applicable in this study as this is a review paper, and we are using secondary published information.

Financial disclosure

This work was supported by the Natural Sciences and Engineering Research Council of Canada (R5467A02).

Data availability statement

Data associated with this scoping review have not been deposited in any public repository. All data used in this article have been referenced herein.

CRediT authorship contribution statement

Margaret S. Harrington: Data curation, Formal analysis, Methodology, Supervision, Writing – original draft, Writing – review & editing. **Stefania D.F. Di Leo:** Data curation, Formal analysis, Investigation, Writing – review & editing. **Courtney A. Hlady:** Formal analysis, Investigation, Writing – review & editing. **Timothy A. Burkhart:** Conceptualization, Funding acquisition, Methodology, Project administration, Resources, Supervision, Writing – review & editing.

Declaration of competing interest

The authors declare that they have no known competing financial interests or personal relationships that could have appeared to influence the work reported in this paper.

Acknowledgments

The authors would like to thank Julia Martyniuk for their valuable support in developing the search strategy. The authors would also like to thank Pratham Singh and Lucy Tempest for their assistance screening the titles, abstracts, and full-text reports for inclusion and exclusion.

Appendix A

Databases were searched twice.

- First search: October 20th, 2021
- Second search: July 3rd, 2023

Table A1
Medline Search Strategy

1	exp Models, Anatomic/or exp computer simulation/or models, neurological/or patient-specific modeling/
2	((neuromuscul* or musculoskeletal or subject-specific or patient-specific) adj 4 (model* or simulat*)).tw,kf.
3	1 or 2
4	Hip/or Hip joint/or exp Femur/or Pelvis/
5	(hip or femur or femoral or pelvi* or acetabul*).tw,kf.
6	4 or 5
7	exp Bone Diseases/or exp Joint Diseases/or exp Musculoskeletal Abnormalities/
8	(deform* or abnormalit* or patholog* or pathomorpholog* or disease* or disorder*).tw,kf.
9	7 or 8
10	3 and 6 and 9
11	Animals/not Humans/
12	10 not 11
13	limit 12 to yr = "1990-Current"

For second search, line 13 was: limit 12 to yr = "2021-Current".

Table A2
Web of Science Search Strategy

1	TS=((neuromuscul* or musculoskeletal or subject-specific or patient-specific) near/3 (model* or simulat*))
2	TS=(hip or femur or femoral or pelvi* or acetabul*)
3	TS=(deform* or abnormalit* or patholog* or pathomorpholog* or disease* or disorder*)
4	1 and 2 and 3
5	TS=(Animal* not Human*)
6	4 not 5
7	Publication date = Jan 1, 1990–Oct 20, 2021

For second search, line 7 was: Publication date = Oct 20, 2021–July 3, 2021

Appendix B

Modified quality assessment checklist originally developed by Moissenet et al. (2017).

Q1 Are the research objectives clearly stated?
Q2 Is the study design clearly described?
Q3 Is the scientific context clearly explained?
Q4 Is the musculoskeletal model adequately described?
Q5 Were the model alterations clearly described?
Q6 Is the model for joint contact force estimation adequately described?
Q7 Were participant characteristics adequately described?
Q8 Were movement tasks, equipment design, and setup clearly defined?
Q9 Were relevant instrumentation specifications and signal processing techniques described?
Q10 Were the statistical methods justified and appropriately described (other than descriptive statistics)?
Q11 Were the direct results easily interpretable?
Q12 Were the main outcomes clearly stated and supported by the results?
Q13 Were the limitations of the study clearly described?
Q14 Were key findings supported by other literature?
Q15 Were conclusions drawn from the study clearly stated?

Table B1
Quality assessment of included studies using a modified checklist developed by Moissenet et al. (2017) for biomechanical research.

Reference	Q1	Q2	Q3	Q4	Q5	Q6	Q7	Q8	Q9	Q10	Q11	Q12	Q13	Q14	Q15	Score (%)
Alexander et al. [58]	2	2	2	2	2	2	1	1	2	1	1	2	2	1	2	83
Bahl et al. [5]	2	2	2	2	1	–	2	2	1	2	1	1	2	2	2	86
Bahl et al. [20]	2	2	2	1	2	1	2	1	1	2	1	2	2	2	2	83
Bosmans et al. [42]	1	2	2	1	2	1	2	2	1	2	1	2	2	2	2	83
Bosmans et al. [43]	1	2	2	1	2	–	2	1	0	2	1	2	2	2	2	79
Buehler et al. [21]	2	2	2	1	1	0	1	2	1	2	1	2	2	1	2	73
Cannon et al. [50]	2	2	2	1	1	1	2	2	2	1	2	2	2	2	2	87
Carriero et al. [44]	2	2	2	1	–	1	1	2	1	–	1	2	2	1	2	77
Catelli et al. [51]	2	2	2	2	2	1	2	2	1	2	2	1	2	2	2	90
Catelli et al. [3]	2	2	2	2	2	1	2	2	1	2	2	2	2	2	2	93
Catelli et al. [52]	2	2	2	2	2	1	1	2	1	2	2	1	2	2	1	83
Choi et al. [45]	1	2	2	1	–	–	2	2	1	1	1	2	1	1	2	73
De Pieri et al. [59]	2	2	2	2	2	2	1	2	1	1	1	2	2	2	1	83
Delp et al. [34]	2	2	2	1	2	–	1	1	1	0	2	2	2	2	2	79
Diamond et al. [22]	2	2	2	2	2	1	2	1	1	2	2	2	2	2	2	90
Foucher et al. [23]	2	2	2	1	–	1	2	2	1	2	2	2	2	1	2	86
Fuller and Winters [24]	2	2	2	1	1	1	1	1	1	1	1	1	2	2	2	70
Gaffney et al. [35]	2	2	2	1	1	1	2	1	1	2	1	2	2	2	2	80
Gaffney et al. [6]	2	2	2	2	2	1	2	1	1	2	2	2	2	2	2	90
Harris et al. [36]	2	2	2	2	1	1	2	2	2	2	2	2	2	2	2	93
Hoang et al. [25]	2	2	2	2	2	1	2	1	1	2	2	1	2	2	2	87
Lenaerts et al. [26]	2	2	2	2	1	1	2	1	1	2	2	2	2	2	2	87
Lenaerts et al. [27]	2	2	2	1	1	1	2	1	1	2	2	1	1	2	2	77
Lenaerts et al. [28]	2	2	2	1	2	1	2	1	1	1	2	2	2	2	2	83
Meyer et al. [29]	2	2	2	1	1	1	2	2	1	2	2	2	1	2	1	80
Modenese et al. [60]	2	2	2	2	0	2	1	1	1	2	2	2	1	2	2	80
Ng et al. [53]	2	2	2	2	1	2	2	2	1	1	2	2	2	2	2	90
Ng et al. [54]	2	2	2	2	1	1	2	2	1	2	2	2	2	2	2	90
Passmore et al. [61]	2	2	2	2	1	2	2	1	1	2	2	2	2	2	1	87
Samaan et al. [55]	2	2	2	2	2	–	2	2	1	2	1	1	2	2	2	89
Savage et al. [56]	1	2	2	2	1	2	2	1	1	2	1	2	2	2	2	83
Scheys et al. [46]	1	2	2	1	2	–	2	1	1	2	1	2	1	2	2	79
Scheys et al. [47]	1	2	2	1	2	–	2	1	1	2	1	2	2	2	1	79
Shepherd et al. [39]	2	2	2	2	2	2	2	2	1	2	1	2	2	2	2	93
Shepherd et al. [40]	2	2	2	2	2	2	2	2	1	2	1	2	2	2	2	93
Song et al. [13]	2	2	2	2	2	1	2	2	1	2	2	2	2	2	2	93
Song et al. [37]	2	2	2	2	2	1	2	2	2	2	1	2	2	2	2	93
Song et al. [38]	2	2	2	1	2	1	2	2	2	2	1	2	2	2	2	90
Song et al. [4]	2	2	2	2	1	2	2	1	2	2	2	2	2	2	2	93
Tateuchi et al. [57]	1	2	2	2	2	1	2	2	1	2	1	2	2	2	2	87
Van Rossom et al. [33]	1	2	2	1	1	2	1	1	1	1	2	2	2	2	2	77
Vandekerckhove et al. [48]	2	2	2	2	2	–	2	1	1	2	2	2	2	2	2	93
Wesseling et al. [30]	1	2	2	2	1	1	2	1	1	0	2	2	2	2	2	77
Wesseling et al. [31]	2	2	2	2	1	1	2	1	1	2	2	1	2	2	2	83
Wesseling et al. [49]	2	2	2	2	2	1	2	1	1	2	2	2	2	1	2	87
Wesseling et al. [32]	2	2	2	1	2	1	2	2	1	–	2	2	2	2	2	89
Wu et al. [41]	1	1	2	1	1	2	2	1	0	1	2	2	2	2	2	73

Appendix C

Template for Reporting Table for Musculoskeletal Modeling Studies.

Topic and Item	Recommendation (*Delete column after description for study has been filled in)*	Description for Study
General Model Information		
1. Name and general details	Name of model (e.g., 2396Hip), citation, number of segments, degrees of freedom, musculotendon units.	
2. Baseline model modifications	Describe any changes to the baseline model cited in item 1 (e.g., changes to range of motion, muscle wrapping surfaces).	
3. Control model	Specify control model used for movement simulations (e.g., static optimization, computed muscle control).	
Instrumentation		
4. Kinematics and kinetics	Specify motion capture and force measurement systems, marker set or inertial measurement locations, sampling rates, filters, and filter cut-off frequencies and justifications for cut-offs.	
5. Electromyography	Report following the standard guidelines[1]: a Electrodes – model, material, shape, size, interelectrode difference, electrode location b Detection and amplification – gain, dynamic range, input impedance and skin preparation, common mode rejection ratio, band-pass filter c Amplitude processing – rectification, smoothing approach (e.g., filter and cut-off frequency, root mean square) d Normalization method	
6. Medical imaging	Describe protocols used to obtain imaging data for model personalization.	
Model Personalization and Simulation Methods		
7. Model personalization	Describe modifications to personalize the baseline model: a Rigid bodies – scaling approach, number of scale factors per segment and landmarks used, statistical shape modeling, image-derived geometry, etc. b Joint centres – generic, image-derived, regression, etc. c Musculotendon units – scaling of maximum isometric muscle forces or muscle and tendon fiber lengths, image-based updates to muscle attachments and paths, etc.	
8. Residual errors	Report residual errors for marker locations during scaling and tracking and for forces and moments.	
Model Validation		
9. Experimental data	Describe participant characteristics, data collection and processing methods for model data and reference data (e.g., instrumented prosthesis, electromyography). Cite validation if not conducted in the current study.	
10. Validation methods and results	Describe methods for quantitative validation (e.g., muscle activation onset comparison, cross-correlation) and specify results. Summarize qualitative validation results.	

1 Merletti, R. Standards for Reporting EMG data. *Journal of Electromyography and Kinesiology*, February 1999; 9 (1):III-IV

References

[1] A. Seth, J.L. Hicks, T.K. Uchida, A. Habib, C.L. Dembia, J.J. Dunne, C.F. Ong, M.S. DeMers, A. Rajagopal, M. Millard, S.R. Hamner, E.M. Arnold, J.R. Yong, S. K. Lakshmikanth, M.A. Sherman, J.P. Ku, S.L. Delp, OpenSim: simulating musculoskeletal dynamics and neuromuscular control to study human and animal movement, PLoS Comput. Biol. 14 (2018), https://doi.org/10.1371/journal.pcbi.1006223.

[2] J.L. Hicks, T.K. Uchida, A. Seth, A. Rajagopal, S.L. Delp, Is my model good enough? Best practices for verification and validation of musculoskeletal models and simulations of movement, J. Biomech. Eng. 137 (2015), https://doi.org/10.1115/1.4029304.

[3] D.S. Catelli, K.C.G. Ng, M. Wesseling, E. Kowalski, I. Jonkers, P.E. Beaulé, M. Lamontagne, Hip muscle forces and contact loading during squatting after cam-type FAI surgery, J. Bone Joint Surg. 102 (2020) 34–42, https://doi.org/10.2106/JBJS.20.00078.

[4] K. Song, C. Pascual-Garrido, J.C. Clohisy, M.D. Harris, Elevated loading at the posterior acetabular edge of dysplastic hips during double-legged squat, J. Orthop. Res. 40 (2022) 2147–2155, https://doi.org/10.1002/jor.25249.

[5] J.S. Bahl, J.B. Arnold, M. Taylor, L.B. Solomon, D. Thewlis, Lower functioning patients demonstrate atypical hip joint loading before and following total hip arthroplasty for osteoarthritis, J. Orthop. Res. 38 (2020) 1550–1558, https://doi.org/10.1002/JOR.24716.

[6] B.M.M. Gaffney, M. Harris-Hayes, J.C. Clohisy, M.D. Harris, Effect of simulated rehabilitation on hip joint loading during single limb squat in patients with hip dysplasia, J. Biomech. 116 (2021), https://doi.org/10.1016/j.jbiomech.2020.110183.

[7] S.D. Uhlrich, T.K. Uchida, M.R. Lee, S.L. Delp, Ten steps to becoming a musculoskeletal simulation expert: a half-century of progress and outlook for the future, J. Biomech. 154 (2023), https://doi.org/10.1016/j.jbiomech.2023.111623.

[8] M.E. Lund, M. De Zee, M.S. Andersen, J. Rasmussen, On validation of multibody musculoskeletal models, in: Proc Inst Mech Eng H, 2012, pp. 82–94, https://doi.org/10.1177/0954411911431516.

[9] J. Holder, U. Trinler, A. Meurer, F. Stief, A systematic review of the associations between inverse dynamics and musculoskeletal modeling to investigate joint loading in a clinical environment, Front. Bioeng. Biotechnol. 8 (2020), https://doi.org/10.3389/fbioe.2020.603907.

[10] F. Moissenet, L. Modenese, R. Dumas, Alterations of musculoskeletal models for a more accurate estimation of lower limb joint contact forces during normal gait: a systematic review, J. Biomech. 63 (2017) 8–20, https://doi.org/10.1016/j.jbiomech.2017.08.025.

[11] M. Silva, B. Freitas, R. Andrade, Ó. Carvalho, D. Renjewski, P. Flores, J. Espregueira-Mendes, Current perspectives on the biomechanical modelling of the human lower limb: a systematic review, Arch. Comput. Methods Eng. 28 (2021) 601–636, https://doi.org/10.1007/s11831-019-09393-1.
[12] A. Rajagopal, C.L. Dembia, M.S. DeMers, D.D. Delp, J.L. Hicks, S.L. Delp, Full body musculoskeletal model for muscle-driven simulation of human gait, IEEE Trans. Biomed. Eng. 63 (2016) 2068, https://doi.org/10.1109/TBME.2016.2586891.
[13] K. Song, A.E. Anderson, J.A. Weiss, M.D. Harris, Musculoskeletal models with generic and subject-specific geometry estimate different joint biomechanics in dysplastic hips, Comput. Methods Biomech. Biomed. Eng. 22 (2019) 259–270, https://doi.org/10.1080/10255842.2018.1550577.
[14] M. Tomasi, A. Artoni, L. Mattei, F. Di Puccio, On the estimation of hip joint loads through musculoskeletal modeling, Biomech. Model. Mechanobiol. 22 (2023) 379–400, https://doi.org/10.1007/s10237-022-01668-0.
[15] J.C. Clohisy, J.A. Keeney, P.L. Schoenecker, Preliminary assessment and treatment guidelines for hip disorders in young adults, in: Clin Orthop Relat Res, Lippincott Williams and Wilkins, 2005, pp. 168–179, https://doi.org/10.1097/01.blo.0000193511.91643.2a.
[16] F. Moissenet, L. Modenese, R. Dumas, Alterations of musculoskeletal models for a more accurate estimation of lower limb joint contact forces during normal gait: a systematic review, J. Biomech. 63 (2017) 8–20, https://doi.org/10.1016/J.JBIOMECH.2017.08.025.
[17] H. Arksey, L. O'Malley, Scoping studies: towards a methodological framework, Int. J. Soc. Res. Methodol.: Theor. Pract. 8 (2005) 19–32, https://doi.org/10.1080/1364557032000119616.
[18] S.L. Delp, J.L. Hicks, A. Seth, A. Habib, C.L. Dembia, S.K. Lakshmikanth, T.K. Uchida, C.F. Ong, J.J. Dunne, OpenSim documentation, Atlas (2024). https://opensimconfluence.atlassian.net/wiki/spaces/OpenSim/overview. (Accessed 18 June 2024).
[19] AnyBody Technology and Anybody Research Group, AnyBody Documentation , AnyScript, 2024. https://anyscript.org/. (Accessed 18 June 2024).
[20] J.S. Bahl, J. Zhang, B.A. Killen, M. Taylor, L.B. Solomon, J.B. Arnold, D.G. Lloyd, T.F. Besier, D. Thewlis, Statistical shape modelling versus linear scaling: effects on predictions of hip joint centre location and muscle moment arms in people with hip osteoarthritis, J. Biomech. 85 (2019) 164–172, https://doi.org/10.1016/j.jbiomech.2019.01.031.
[21] C. Buehler, W. Koller, F. De Comtes, H. Kainz, Quantifying muscle forces and joint loading during hip exercises performed with and without an elastic resistance band, Front Sports Act Living 3 (2021), https://doi.org/10.3389/fspor.2021.695383.
[22] L.E. Diamond, H.X. Hoang, R.S. Barrett, A. Loureiro, M. Constantinou, D.G. Lloyd, C. Pizzolato, Individuals with mild-to-moderate hip osteoarthritis walk with lower hip joint contact forces despite higher levels of muscle co-contraction compared to healthy individuals, Osteoarthritis Cartilage 28 (2020) 924–931, https://doi.org/10.1016/j.joca.2020.04.008.
[23] K.C. Foucher, D.E. Hurwitz, M.A. Wimmer, Do gait adaptations during stair climbing result in changes in implant forces in subjects with total hip replacements compared to normal subjects? Clin. BioMech. 23 (2008) 754–761, https://doi.org/10.1016/j.clinbiomech.2008.02.006.
[24] J.J. Fuller, J.M. Winters, Assessment of 3-D Joint Contact Load Predictions during Posturai/Stretching Exercises in Aged Females, 1993.
[25] H.X. Hoang, L.E. Diamond, D.G. Lloyd, C. Pizzolato, A calibrated EMG-informed neuromusculoskeletal model can appropriately account for muscle co-contraction in the estimation of hip joint contact forces in people with hip osteoarthritis, J. Biomech. 83 (2019) 134–142, https://doi.org/10.1016/j.jbiomech.2018.11.042.
[26] G. Lenaerts, F. De Groote, B. Demeulenaere, M. Mulier, G. Van der Perre, A. Spaepen, I. Jonkers, Subject-specific hip geometry affects predicted hip joint contact forces during gait, J. Biomech. 41 (2008) 1243–1252, https://doi.org/10.1016/j.jbiomech.2008.01.014.
[27] G. Lenaerts, W. Bartels, F. Gelaude, M. Mulier, A. Spaepen, G. Van der Perre, I. Jonkers, Subject-specific hip geometry and hip joint centre location affects calculated contact forces at the hip during gait, J. Biomech. (2009), https://doi.org/10.1016/j.jbiomech.2009.03.037.
[28] G. Lenaerts, M. Mulier, A. Spaepen, G. Van der Perre, I. Jonkers, Aberrant pelvis and hip kinematics impair hip loading before and after total hip replacement, Gait Posture 30 (2009) 296–302, https://doi.org/10.1016/j.gaitpost.2009.05.016.
[29] C.A.G. Meyer, M. Wesseling, K. Corten, A. Nieuwenhuys, D. Monari, J.P. Simon, I. Jonkers, K. Desloovere, Hip movement pathomechanics of patients with hip osteoarthritis aim at reducing hip joint loading on the osteoarthritic side, Gait Posture 59 (2018) 11–17, https://doi.org/10.1016/j.gaitpost.2017.09.020.
[30] M. Wesseling, F. De Groote, C. Meyer, K. Corten, J.-P. Simon, K. Desloovere, I. Jonkers, Subject-specific musculoskeletal modelling in patients before and after total hip arthroplasty*, Comput. Methods Biomech. Biomed. Eng. 19 (2016) 1683–1691, https://doi.org/10.1080/10255842.2016.1181174.
[31] M. Wesseling, C. Meyer, K. Corten, K. Desloovere, I. Jonkers, Longitudinal joint loading in patients before and up to one year after unilateral total hip arthroplasty, Gait Posture 61 (2018) 117–124, https://doi.org/10.1016/J.GAITPOST.2018.01.002.
[32] M. Wesseling, S. Van Rossom, I. Jonkers, C.R. Henak, Subject-specific geometry affects acetabular contact pressure during gait more than subject-specific loading patterns, Comput. Methods Biomech. Biomed. Eng. 22 (2019) 1323–1333, https://doi.org/10.1080/10255842.2019.1661393.
[33] S. Van Rossom, J. Emmerzaal, R. van der Straaten, M. Wesseling, K. Corten, J. Bellemans, J. Truijen, J. Malcorps, A. Timmermans, B. Vanwanseele, I. Jonkers, The biomechanical fingerprint of hip and knee osteoarthritis patients during activities of daily living, Clin. BioMech. 101 (2023), https://doi.org/10.1016/j.clinbiomech.2022.105858.
[34] S.L. Delp, E.E. Bleck, F.E. Zajac, G. Bollini, Biomechanical analysis of the Chiari pelvic osteotomy. Preserving hip abductor strength, Clin. Orthop. Relat. Res. 254 (1990) 189–198. NS -.
[35] B.M.M. Gaffney, J.C. Clohisy, L.R. Van Dillen, M.D. Harris, The association between periacetabular osteotomy reorientation and hip joint reaction forces in two subgroups of acetabular dysplasia, J. Biomech. 98 (2020) 109464, https://doi.org/10.1016/J.JBIOMECH.2019.109464.
[36] M.D. Harris, B.A. MacWilliams, K. Bo Foreman, C.L. Peters, J.A. Weiss, A.E. Anderson, Higher medially-directed joint reaction forces are a characteristic of dysplastic hips: a comparative study using subject-specific musculoskeletal models, J. Biomech. 54 (2017) 80–87, https://doi.org/10.1016/j.jbiomech.2017.01.040.
[37] K. Song, B.M.M. Gaffney, K.B. Shelburne, C. Pascual-Garrido, J.C. Clohisy, M.D. Harris, Dysplastic hip anatomy alters muscle moment arm lengths, lines of action, and contributions to joint reaction forces during gait, J. Biomech. 110 (2020), https://doi.org/10.1016/j.jbiomech.2020.109968.
[38] K. Song, C. Pascual-Garrido, J.C. Clohisy, M.D. Harris, Acetabular edge loading during gait is elevated by the anatomical deformities of hip dysplasia, Front Sports Act Living 3 (2021), https://doi.org/10.3389/fspor.2021.687419.
[39] M.C. Shepherd, B.M.M. Gaffney, K. Song, J.C. Clohisy, J.J. Nepple, M.D. Harris, Femoral version deformities alter joint reaction forces in dysplastic hips during gait, J. Biomech. 135 (2022), https://doi.org/10.1016/j.jbiomech.2022.111023.
[40] M.C. Shepherd, J.C. Clohisy, J.J. Nepple, M.D. Harris, Derotational femoral osteotomy locations and their influence on joint reaction forces in dysplastic hips, J. Orthop. Res. (2023), https://doi.org/10.1002/jor.25559.
[41] T. Wu, K.R. Lohse, L. Van Dillen, K. Song Phd, J.C. Clohisy, M.D. Harris, Are abnormal muscle biomechanics and patient-reported outcomes associated in patients with hip dysplasia? Clin. Orthop. Relat. Res. (2023) 1–10, https://doi.org/10.1097/CORR.0000000000002728, 00.
[42] L. Bosmans, M. Wesseling, K. Desloovere, G. Molenaers, L. Scheys, I. Jonkers, Hip contact force in presence of aberrant bone geometry during normal and pathological gait, J. Orthop. Res. 32 (2014) 1406–1415, https://doi.org/10.1002/jor.22698.
[43] L. Bosmans, K. Jansen, M. Wesseling, G. Molenaers, L. Scheys, I. Jonkers, The role of altered proximal femoral geometry in impaired pelvis stability and hip control during CP gait: a simulation study, Gait Posture 44 (2016) 61–67, https://doi.org/10.1016/j.gaitpost.2015.11.010.
[44] A. Carriero, A. Zavatsky, J. Stebbins, T. Theologis, G. Lenaerts, I. Jonkers, S.J. Shefelbine, Influence of altered gait patterns on the hip joint contact forces, Comput. Methods Biomech. Biomed. Eng. 17 (2014) 352–359, https://doi.org/10.1080/10255842.2012.683575.
[45] S.J. Choi, C.Y. Chung, K.M. Lee, D.G. Kwon, S.H. Lee, M.S. Park, Validity of gait parameters for hip flexor contracture in patients with cerebral palsy, J. NeuroEng. Rehabil. 8 (2011), https://doi.org/10.1186/1743-0003-8-4.
[46] L. Scheys, A. Van Campenhout, A. Spaepen, P. Suetens, I. Jonkers, Personalized MR-based musculoskeletal models compared to rescaled generic models in the presence of increased femoral anteversion: effect on hip moment arm lengths, Gait Posture 28 (2008) 358–365, https://doi.org/10.1016/j.gaitpost.2008.05.002.
[47] L. Scheys, K. Desloovere, P. Suetens, I. Jonkers, Level of subject-specific detail in musculoskeletal models affects hip moment arm length calculation during gait in pediatric subjects with increased femoral anteversion, J. Biomech. 44 (2011) 1346–1353, https://doi.org/10.1016/j.jbiomech.2011.01.001.

[48] I. Vandekerckhove, M. Wesseling, H. Kainz, K. Desloovere, I. Jonkers, The effect of hip muscle weakness and femoral bony deformities on gait performance, Gait Posture 83 (2021) 280–286, https://doi.org/10.1016/j.gaitpost.2020.10.022.

[49] M. Wesseling, L. Bosmans, C. Van Dijck, J. Vander Sloten, R. Wirix-Speetjens, I. Jonkers, Non-rigid deformation to include subject-specific detail in musculoskeletal models of CP children with proximal femoral deformity and its effect on muscle and contact forces during gait, Comput. Methods Biomech. Biomed. Eng. 22 (2019), https://doi.org/10.1080/10255842.2018.1558216.

[50] J. Cannon, K. Kulig, A.E. Weber, C.M. Powers, Gluteal activation during squatting reduces acetabular contact pressure in persons with femoroacetabular impingement syndrome: a patient-specific finite element analysis, Clin. BioMech. 101 (2023), https://doi.org/10.1016/J.CLINBIOMECH.2022.105849.

[51] D.S. Catelli, K.C.G. Ng, E. Kowalski, P.E. Beaulé, M. Lamontagne, Modified gait patterns due to cam FAI syndrome remain unchanged after surgery, Gait Posture 72 (2019) 135–141, https://doi.org/10.1016/j.gaitpost.2019.06.003.

[52] D.S. Catelli, B.L.S. Bedo, P.E. Beaulé, M. Lamontagne, Pre- and postoperative in silico biomechanics in individuals with cam morphology during stair tasks, Clin. BioMech. 86 (2021), https://doi.org/10.1016/j.clinbiomech.2021.105387.

[53] K.C.G. Ng, G. Mantovani, M. Lamontagne, M.R. Labrosse, P.E. Beaulé, Increased hip stresses resulting from a cam deformity and decreased femoral neck-shaft angle during level walking, Clin. Orthop. Relat. Res. 475 (2017) 998–1008, https://doi.org/10.1007/S11999-016-5038-2.

[54] K.C.G. Ng, G. Mantovani, L. Modenese, P.E. Beaulé, M. Lamontagne, Altered walking and muscle patterns reduce hip contact forces in individuals with symptomatic cam femoroacetabular impingement, Am. J. Sports Med. 46 (2018) 2615–2623, https://doi.org/10.1177/0363546518787518.

[55] M.A. Samaan, A.L. Zhang, T. Popovic, V. Pedoia, S. Majumdar, R.B. Souza, Hip joint muscle forces during gait in patients with femoroacetabular impingement syndrome are associated with patient reported outcomes and cartilage composition, J. Biomech. 84 (2019) 138–146, https://doi.org/10.1016/j.jbiomech.2018.12.026.

[56] T.N. Savage, D.J. Saxby, D.G. Lloyd, H.X. Hoang, E.K. Suwarganda, T.F. Besier, L.E. Diamond, J. Eyles, C. Fary, M. Hall, R. Molnar, N.J. Murphy, J. O'donnell, L. Spiers, P. Tran, T.V. Wrigley, K.L. Bennell, D.J. Hunter, C. Pizzolato, Hip contact force magnitude and regional loading patterns are altered in those with femoroacetabular impingement syndrome, Med. Sci. Sports Exerc. 54 (2022) 1831–1841, https://doi.org/10.1249/MSS.0000000000002971.

[57] H. Tateuchi, M. Yamagata, A. Asayama, N. Ichihashi, Influence of simulated hip muscle weakness on hip joint forces during deep squatting, J. Sports Sci. (2021), https://doi.org/10.1080/02640414.2021.1929009.

[58] N. Alexander, R. Brunner, J. Cip, E. Viehweger, E. De Pieri, Increased femoral anteversion does not lead to increased joint forces during gait in a cohort of adolescent patients, Front. Bioeng. Biotechnol. 10 (2022), https://doi.org/10.3389/fbioe.2022.914990.

[59] E. De Pieri, B. Friesenbichler, R. List, S. Monn, N.C. Casartelli, M. Leunig, S.J. Ferguson, Subject-specific modeling of femoral torsion influences the prediction of hip loading during gait in asymptomatic adults, Front. Bioeng. Biotechnol. 9 (2021), https://doi.org/10.3389/fbioe.2021.679360.

[60] L. Modenese, M. Barzan, C.P. Carty, Dependency of lower limb joint reaction forces on femoral version, Gait Posture 88 (2021), https://doi.org/10.1016/j.gaitpost.2021.06.014.

[61] E. Passmore, H.K. Graham, M.G. Pandy, M. Sangeux, Hip- and patellofemoral-joint loading during gait are increased in children with idiopathic torsional deformities, Gait Posture 63 (2018) 228–235, https://doi.org/10.1016/j.gaitpost.2018.05.003.

[62] S.L. Delp, J.P. Loan, M.G. Hoy, F.E. Zajac, E.L. Topp, J.M. Rosen, An interactive graphics-based model of the lower extremity to study orthopaedic surgical procedures, IEEE Trans. Biomed. Eng. 37 (1990) 757–767, https://doi.org/10.1109/10.102791.

[63] V. Carbone, R. Fluit, P. Pellikaan, M.M. van der Krogt, D. Janssen, M. Damsgaard, L. Vigneron, T. Feilkas, H.F.J.M. Koopman, N. Verdonschot, Tlem 2.0 - a comprehensive musculoskeletal geometry dataset for subject-specific modeling of lower extremity, J. Biomech. 48 (2015), https://doi.org/10.1016/j.jbiomech.2014.12.034.

[64] S.R. Hamner, A. Seth, S.L. Delp, Muscle contributions to propulsion and support during running, J. Biomech. 43 (2010), https://doi.org/10.1016/j.jbiomech.2010.06.025.

[65] K. Shelburne, M. Decker, J. Krong, M. Torry, M.J. Philippon, Muscle Forces at the Hip during Squatting Exercise, 56th Annual Meteing of the Orthopaedic Research Society, New Orleans, LA, 2010.

[66] D. Thelen, A. Seth, F.C. Anderson, S.L. Delp, Gait 2392 and 2354 models, OpenSim Documentation, https://simtk-confluence.stanford.edu:8443/display/OpenSim/Gait+2392+and+2354+Models, 2012. (Accessed 2 July 2023).

[67] G.T. Yamaguchi, F.E. Zajac, A PLANAR MODEL OF THE KNEE JOINT TO CHARACTERIZE THE KNEE EXTENSOR MECHANISM, 1989.

[68] G.G. Handsfield, C.H. Meyer, J.M. Hart, M.F. Abel, S.S. Blemker, Relationships of 35 lower limb muscles to height and body mass quantified using MRI, J. Biomech. 47 (2014) 631–638, https://doi.org/10.1016/j.jbiomech.2013.12.002.

[69] S.A. Roelker, E.J. Caruthers, R.K. Hall, N.C. Pelz, A.M.W. Chaudhari, R.A. Siston, Effects of optimization technique on simulated muscle activations and forces, J. Appl. Biomech. 36 (2020) 217–227, https://doi.org/10.1123/JAB.2018-0332.

[70] C. Pizzolato, D.G. Lloyd, M. Sartori, E. Ceseracciu, T.F. Besier, B.J. Fregly, M. Reggiani, CEINMS: a toolbox to investigate the influence of different neural control solutions on the prediction of muscle excitation and joint moments during dynamic motor tasks, J. Biomech. 48 (2015) 3929–3936, https://doi.org/10.1016/j.jbiomech.2015.09.021.

[71] D.S. Catelli, M. Wesseling, I. Jonkers, M. Lamontagne, A musculoskeletal model customized for squatting task, Comput. Methods Biomech. Biomed. Eng. 22 (2019), https://doi.org/10.1080/10255842.2018.1523396.

[72] A.K.M. Lai, A.S. Arnold, J.M. Wakeling, Why are antagonist muscles Co-activated in my simulation? A musculoskeletal model for analysing human locomotor tasks, Ann. Biomed. Eng. 45 (2017), https://doi.org/10.1007/s10439-017-1920-7.

[73] M.Q. Liu, F.C. Anderson, M.H. Schwartz, S.L. Delp, Muscle contributions to support and progression over a range of walking speeds, J. Biomech. 41 (2008) 3243–3252, https://doi.org/10.1016/j.jbiomech.2008.07.031.

[74] G. Bergmann, A. Bender, J. Dymke, G. Duda, P. Damm, Standardized loads acting in hip implants, PLoS One 11 (2016), https://doi.org/10.1371/journal.pone.0155612.

[75] G. Bergmann, G. Deuretzbacher, M. Heller, F. Graichen, A. Rohlmann, J. Strauss, G.N. Duda, Hip contact forces and gait patterns from routine activities, J. Biomech. (2001), https://doi.org/10.1016/S0021-9290(01)00040-9.

[76] M.S. Harrington, T.A. Burkhart, Validation of a musculoskeletal model to investigate hip joint mechanics in response to dynamic multiplanar tasks, J. Biomech. 158 (2023), https://doi.org/10.1016/j.jbiomech.2023.111767.

[77] B.A. Killen, S. Brito da Luz, D.G. Lloyd, A.D. Carleton, J. Zhang, T.F. Besier, D.J. Saxby, Automated creation and tuning of personalised muscle paths for OpenSim musculoskeletal models of the knee joint, Biomech. Model. Mechanobiol. 20 (2021) 521–533, https://doi.org/10.1007/s10237-020-01398-1.

[78] I. Benemerito, E. Montefiori, A. Marzo, C. Mazzà, Reducing the complexity of musculoskeletal models using Gaussian process emulators, Appl. Sci. 12 (2022), https://doi.org/10.3390/app122412932.

[79] F.C. Anderson, M.G. Pandy, Static and dynamic optimization solutions for gait are practically equivalent, J. Biomech. 34 (2001), https://doi.org/10.1016/S0021-9290(00)00155-X.

[80] G. Mantovani, M. Lamontagne, How Different Marker Sets Affect Joint Angles in Inverse Kinematics Framework, 2017, https://doi.org/10.1115/1.4034708.

[81] M.G. Benedetti, A. Merlo, A. Leardini, Inter-laboratory consistency of gait analysis measurements, Gait Posture 38 (2013), https://doi.org/10.1016/j.gaitpost.2013.04.022.

[82] K. Kaufman, E. Miller, T. Kingsbury, E. Russell Esposito, E. Wolf, J. Wilken, M. Wyatt, Reliability of 3D gait data across multiple laboratories, Gait Posture 49 (2016), https://doi.org/10.1016/j.gaitpost.2016.07.075.

[83] S.S. Tomescu, R. Bakker, T.A.C. Beach, N. Chandrashekar, The effects of filter cutoff frequency on musculoskeletal simulations of high-impact movements, J. Appl. Biomech. 34 (2018) 336–341, https://doi.org/10.1123/jab.2017-0145.

[84] C.R. Carvalho, J.M. Fernández, A.J. del-Ama, F. Oliveira Barroso, J.C. Moreno, Review of electromyography onset detection methods for real-time control of robotic exoskeletons, J. NeuroEng. Rehabil. 20 (2023), https://doi.org/10.1186/s12984-023-01268-8.

[85] J. Kaiser, A. Monawer, R. Chaudhary, K.M. Johnson, O. Wieben, R. Kijowski, D.G. Thelen, Accuracy of model-based tracking of knee kinematics and cartilage contact measured by dynamic volumetric MRI, Med. Eng. Phys. 38 (2016) 1131–1135, https://doi.org/10.1016/j.medengphy.2016.06.016.

[86] S.D. Uhlrich, R.W. Jackson, A. Seth, J.A. Kolesar, S.L. Delp, Muscle coordination retraining inspired by musculoskeletal simulations reduces knee contact force, Sci. Rep. 12 (2022), https://doi.org/10.1038/s41598-022-13386-9.
[87] R.M. Kanko, E.K. Laende, E.M. Davis, W.S. Selbie, K.J. Deluzio, Concurrent assessment of gait kinematics using marker-based and markerless motion capture, J. Biomech. 127 (2021), https://doi.org/10.1016/j.jbiomech.2021.110665.
[88] P.B. Shull, W. Jirattigalachote, M.A. Hunt, M.R. Cutkosky, S.L. Delp, Quantified self and human movement: a review on the clinical impact of wearable sensing and feedback for gait analysis and intervention, Gait Posture 40 (2014) 11–19, https://doi.org/10.1016/j.gaitpost.2014.03.189.
[89] D.J. Saxby, B.A. Killen, C. Pizzolato, C.P. Carty, L.E. Diamond, L. Modenese, J. Fernandez, G. Davico, M. Barzan, G. Lenton, S.B. da Luz, E. Suwarganda, D. Devaprakash, R.K. Korhonen, J.A. Alderson, T.F. Besier, R.S. Barrett, D.G. Lloyd, Machine learning methods to support personalized neuromusculoskeletal modelling, Biomech. Model. Mechanobiol. 19 (2020) 1169–1185, https://doi.org/10.1007/s10237-020-01367-8.